



HAL
open science

Differences in Alimentary Glucose 1 Absorption and Intestinal Disposal of Blood Glucose Following Roux-en-Y Gastric Bypass vs Sleeve Gastrectomy

Jean-Baptiste Cavin, Anne Couvelard, Rachida Lebtahi, Robert Ducroc, Konstantinos Arapis, Eglantine Voitellier, Françoise Cluzeaud, Laura Gillard, Muriel Hourseau, Nidaa Mikail, et al.

► To cite this version:

Jean-Baptiste Cavin, Anne Couvelard, Rachida Lebtahi, Robert Ducroc, Konstantinos Arapis, et al.. Differences in Alimentary Glucose 1 Absorption and Intestinal Disposal of Blood Glucose Following Roux-en-Y Gastric Bypass vs Sleeve Gastrectomy: Intestinal glucose handling after bariatric surgery . Gastroenterology, 2015, 150 (2), pp.454-64. 10.1053/j.gastro.2015.10.009 . inserm-01346236

HAL Id: inserm-01346236

<https://inserm.hal.science/inserm-01346236>

Submitted on 18 Jul 2016

HAL is a multi-disciplinary open access archive for the deposit and dissemination of scientific research documents, whether they are published or not. The documents may come from teaching and research institutions in France or abroad, or from public or private research centers.

L'archive ouverte pluridisciplinaire **HAL**, est destinée au dépôt et à la diffusion de documents scientifiques de niveau recherche, publiés ou non, émanant des établissements d'enseignement et de recherche français ou étrangers, des laboratoires publics ou privés.

1 **Differences in Alimentary Glucose Absorption and Intestinal Disposal of Blood**
2 **Glucose Following Roux-en-Y Gastric Bypass vs Sleeve Gastrectomy**

3

4 Short title: Intestinal glucose handling after bariatric surgery

5

6 Jean-Baptiste Cavin¹, Anne Couvelard^{1,2}, Rachida Lebtahi³, Robert Ducroc¹, Konstantinos Arapis^{1,4},
7 Eglantine Voitellier¹, Françoise Cluzeaud¹, Laura Gillard¹, Muriel Hourseau², Nidaa Mikail³, Lara
8 Ribeiro-Parenti⁴, Nathalie Kapel⁵, Jean-Pierre Marmuse^{4,6}, André Bado^{1,6}, Maude Le Gall¹

9

10 ¹INSERM U1149, DHU Unity, Paris Diderot University, 75018, France

11 ²Department of Pathology, Bichat hospital, AP-HP, Paris, 75018, France

12 ³Department of Nuclear Medicine, Bichat hospital, AP-HP, Paris 75018, France

13 ⁴Department of general and digestive surgery, Bichat hospital, AP-HP, Paris 75018, France

14 ⁵Functional Coprology Service, Pitié Salpêtrière Hospital Group, AP-HP, Paris, 75013, France

15 ⁶Co-senior author

16

17 This work was supported by French minister of higher education and research, INSERM and
18 University Paris Diderot.

19

20 BPL, bilio-pancreatic limb; GIP, glucose-dependent insulintropic peptide; GLP1, glucagon-like
21 peptide-1; GLUT, glucose transporter; RL, Roux limb; RYGB, Roux-en-Y gastric bypass; VSG,
22 vertical sleeve gastrectomy; SGLT1, sodium/glucose cotransporter 1; PET/CT, positron emission and
23 computed tomography.

24

25

26 **Corresponding author:**

27 Maude Le Gall Ph.D.

28 Gastrointestinal and Metabolic Dysfunctions in Nutritional Pathologies

29 Centre de Recherche sur l'Inflammation Paris Montmartre

30 Inserm UMRS 1149, Université Paris Diderot Paris 7,

31 Faculté de Médecine Site Bichat

32 16, rue Henri Huchard,

33 75890 Paris Cedex 18, France

34 Email:maude.le-gall@inserm.fr

35 Tel: +33 (0)157 277 459

36 Fax: +33 (0)157 277 471

37

38 The authors have declared that no conflict of interest exists

39

40 **AUTHOR CONTRIBUTIONS**

41 J.-B.C., M.L.G., A.B. and J.-P.M. designed the experiments; J.-B.C., M.L.G., A.B., F.C. and

42 L.G. performed experiments; K.A. and E.V. performed animal surgeries; M.H., supervised by

43 A.C., performed histologic analyses; N.M., supervised by R.L., performed PET/CT scan

44 analyses; N.K. supervised stool analyses; R.D and J.-B.C. performed Ussing chamber

45 analyses; J.-P.M., K.A. and L.R.-P. collected human clinical data and samples; J.-B.C.,

46 M.L.G., A.B., A.C., R.L. analysed and interpreted data; J.-P.M. supervised the human

47 studies; J.-B.C., M.L.G. and A.B. wrote the manuscript with comments from A.C., R.D. and

48 R.L.

49

50 **KEY WORDS:** intestinal adaptation; enteroendocrine cells; enterohormones; GIP

51

52 **ABSTRACT**

53 **Background & Aims:** Bariatric surgeries, such as Roux-en-Y gastric bypass (RYGB) or
54 vertical sleeve gastrectomy (VSG), are the most effective approaches to resolve type 2
55 diabetes in obese individuals. Alimentary glucose absorption and intestinal disposal of blood
56 glucose have not been directly compared between individuals or animals that underwent
57 RYGB vs VSG. We evaluated in rats and humans how the gut epithelium adapts following
58 surgery and the consequences on alimentary glucose absorption and intestinal disposal of
59 blood glucose.

60 **Methods:** Obese male rats underwent RYGB, VSG, or sham (control) surgeries. We
61 collected intestine segments from all rats; we performed histologic analyses and measured
62 levels of mRNAs encoding the sugar transporters SGLT1, GLUT1, GLUT2, GLUT3, GLUT4
63 and GLUT5. Glucose transport and consumption were assayed using ex vivo jejunal loops.
64 Histologic analyses were also performed on Roux limb sections from patients who underwent
65 RYGB, 1–5 years after surgery. Roux limb glucose consumption was assayed following
66 surgery by positron emission and computed tomography imaging.

67 **Results:** In rats and humans that underwent RYGB, the Roux limb became hyperplasic, with
68 an increased number of incretin-producing cells, compared with the corresponding jejunal
69 segment of controls. Furthermore, expression of sugar transporters and hypoxia-related
70 genes increased and the non-intestinal glucose transporter GLUT1 appeared at the
71 basolateral membrane of enterocytes. Ingested and circulating glucose was trapped within
72 the intestinal epithelial cells of rats and humans that underwent RYGB. By contrast, there
73 was no hyperplasia of the intestine after VSG, but the intestinal absorption of alimentary
74 glucose was reduced and density of endocrine cells secreting glucagon-like peptide-1
75 (GLP1) increased.

76 **Conclusions:** The intestine adapts differently to RYGB vs VSG. RYGB increases intestinal
77 glucose disposal, whereas VSG delays glucose absorption; both contribute to observed
78 improvements in glycemia.

80 INTRODUCTION

81 The resolution of type 2 diabetes by bariatric surgery has attracted considerable attention in
82 recent years. Diabetes resolves rapidly after Roux-en-Y Gastric Bypass (RYGB) or Vertical
83 Sleeve Gastrectomy (VSG) ¹. Beyond postoperative weight loss, the surgical procedures
84 themselves contribute to the cure of type 2 diabetes ²⁻⁵. The described mechanisms so far
85 involve caloric restriction ⁶⁻⁸, hormonal changes ^{9 10}, accelerated gastric emptying ¹¹⁻¹³ and
86 bile acid signalling ⁹ but we still lack a clear understanding of the underpinning mechanisms.
87 The gastrointestinal tract is the direct target of bariatric surgeries, and the early intestinal
88 remodeling and adaptation triggered by such interventions could be the starting point for
89 metabolic improvement ¹³. Unquestionably, the small intestine contributes to glycemic control
90 by orchestrating glucose transfer to the portal circulation after breakdown of complex
91 carbohydrates to glucose. In addition, the gastrointestinal tract is an important endocrine
92 organ with enteroendocrine cells secreting gut hormones, *i.e.*, Glucagon-Like Peptide 1
93 (GLP1) and glucose-dependent Insulinotropic Peptide (GIP), involved in glucose-induced
94 insulin secretion ¹⁴. Most hypotheses propose that after RYGB, accelerated deliveries of
95 nutrients to the distal gut, as well as duodenal exclusion, contribute to alterations in
96 circulating gut hormone concentrations and improvement in glucose homeostasis ¹⁵.
97 The remodeling of gastrointestinal tract after RYGB surgery has been extensively studied in
98 rat models and hyperplasia of the alimentary Roux limb (RL) was described in most reports
99 ¹⁶⁻²¹. This hyperplasia was associated with a reprogramming of intestinal glucose metabolism
100 toward an increased glucose consumption to support tissue growth in a rat model of RYGB
101 ^{19,21}. These recent observations contrast with previous studies reporting either a reduction in
102 glucose uptake from the intestinal lumen ²² or no changes in intestinal glucose uptake *ex vivo*
103 ²³. In addition, results of the literature regarding the expression pattern of intestinal sugar
104 transporters after surgery are heterogeneous ^{17,19,22,24}. Glucose handling by the intestine is
105 actually compartmentalized in two functional circuits: during the meals, alimentary glucose is
106 absorbed and transferred to the portal blood, whereas at the fasted state, some glucose is

107 taken up from the arterial blood and used for intestinal metabolism ²⁵. Previous studies focus
108 only on parts of this complex process, thus it remains unclear how the remodeled intestine
109 absorbs and consumes alimentary and blood glucose after RYGB. One recent publication
110 reported no hyperplasia of the jejunum and no reprogramming of intestinal glucose
111 metabolism after SVG ²¹, however no study truly investigates the consequences of VSG on
112 intestinal glucose handling.

113 In this study, we directly compared and contrasted the impact of RYGB and VSG surgeries
114 on glucose handling by the intestine, distinguishing alimentary glucose transport from blood
115 glucose intestinal uptake. In diet-induced obese rat models, the two surgeries differently alter
116 intestinal morphology, enteroendocrine cell differentiation and glucose handling by the
117 intestine in ways favourable for the regulation of glucose homeostasis. Finally, we extended
118 our most important results to humans demonstrating that RYGB induces hypertrophy of the
119 alimentary Roux limb with an increased number of incretin-producing cells and an unusual
120 overexpression of the glucose transporter GLUT1 associated with a hypermetabolic activity
121 of the epithelial cells.

122

123 **MATERIALS AND METHODS**

124 See Supplemental Experimental Procedures for detailed descriptions.

125 **Animal surgeries and post-surgery procedures**

126 All animal use conformed to the European Community guidelines was approved by the local
127 ethics committee (N°#2011-14/773-0030 Comité d'Ethique Paris-Nord) and the Ministry of
128 Higher Education and Research (N° 02285.01). Diet-induced obese rats were operated from
129 Roux-en-Y gastric bypass (RYGB), sleeve gastrectomy (VSG) or sham surgery (sham) as
130 previously described ²⁶.

131 **Human jejunal samples**

132 Eight patients treated by surgery from November 2013 to July 2015 were retrospectively
133 selected from the files of the department of pathology, Bichat Hospital, France. Mean age
134 was 46.8±12.7 years at the time of the surgery and BMI was 55±5.6 for obese control group
135 (n = 3) and 35.9±4.8 for RYGB patients (n = 5). None of them were diabetic and they had no
136 medication to control their glycemia (See table S1).

137 **Positron emission tomography**

138 Seven patients were retrospectively selected from the files of the department of nuclear
139 medicine, Bichat Hospital, France. Three RYGB patients and four control patients (without
140 gastro-intestinal diseases or cancer) had been evaluated with [18F]-FDG PET/CT. In the
141 RYGB group, mean age was 55.7 ± 7.6; BMI was 29.6 ± 3.2, in the control group, mean age
142 was 64.5 ± 14.4; BMI was 30.6 ± 4.2; none of them were diabetic and they had no
143 medication to control their glycaemia. PET and CT were performed with a PET/CT hybrid
144 system (Discovery 690; GE Healthcare). See table S2 and Supplemental Experimental
145 Procedures for detailed description of patients, procedure and image analyses.

146 **Statistical analyses**

147 All values are expressed as mean ± SEM. One-way ANOVA with Bonferroni correction for
148 multiple comparisons were used to compare more than 2 groups and non-parametric Mann-
149 Whitney tests were used to compare 2 groups. P < 0.05 was considered to be significant.

150 **RESULTS**

151 ***RYGB quickly induces hypertrophy of the alimentary Roux limb***

152 We studied early events following RYGB surgery either in a diet-induced obese rat model
153 (Text S1 and Figure S2). As soon as 2 weeks after surgery, the alimentary Roux limb (RL)
154 was hypertrophic and displayed a dramatic increase in its diameter compared with that of the
155 biliopancreatic limb (BPL) or with the corresponding jejunal segment (Jej) of sham-operated
156 rats (Figure 1A). The villus height and crypt depth of the RL were increased leading to a
157 thicker mucosa, whereas no modification of the BPL was observed (Figure 1B). The increase
158 in average mucosal area was maintained over 40 days (Figure S3A). Moreover, the crypt
159 cells in the hyperplastic RL were highly proliferative, as evidenced by the dense Ki67
160 immunostaining of mucosa (Figure 1C) and the increase in the number of Ki67-positive cells
161 (Figure 1D).

162 Remarkably, in humans, the RL was hypertrophic with obvious increase in mucosal area
163 (Figure 1E), increase in crypt depth ($241 \pm 37 \mu\text{m}$ vs $163 \pm 10 \mu\text{m}$ in control group), but no
164 changes in villus height ($674 \pm 35 \mu\text{m}$ vs $705 \pm 16 \mu\text{m}$ in control group). The number of Ki67-
165 positive cells was also increased (51 ± 7 cells/crypt vs 38 ± 1 cells/crypt in control group)
166 (Figure 1F).

167

168 ***Increased number of endocrine cells in the hypertrophic alimentary Roux limb***

169 A direct consequence of RL overgrowth was a local increased in the number of glucagon-
170 like peptide (GLP1) (Figure 2A and 2B) and glucose-dependent insulinotropic peptide (GIP)
171 producing cells (Figure 2C). Accordingly, glucose-induced GLP1 secretion increased (Figure
172 S4). However, there were no significant changes in the average density of those
173 enteroendocrine cells (Figure 2B and 2C). The same observations were made in RL from
174 RYGB humans where no variation was found in the average density of enteroendocrine cells
175 (*i.e.*, Chromogranin A-positive cells) or GLP1 secreting cells (Figure 2D and 2E).

176

177 **Early and unusual expression of the glucose transporter GLUT1 in the alimentary**

178 **Roux limb**

179 We investigated the expression of various sugar transporters in the hyperplastic RL (Figure
180 3A and 3B) and the non-hyperplastic BPL (Figure S5A and S5B) after RYGB surgery in rats.
181 Expression of genes encoding the prevalent intestinal transporters, *i.e.*, sodium-dependent
182 glucose co-transporter 1 (SGLT1), and facilitative glucose transporter GLUT2 were not
183 significantly increased two weeks after surgery whereas expression of fructose transporter
184 GLUT5 tended to decrease (Figure 3A). However, SGLT1 transport activity measured in
185 Ussing chamber doubled in the RL at 14 days ($\Delta I_{sc} = 5.3 \pm 0.5 \mu A/cm^2$ in sham *versus* ΔI_{sc}
186 $= 16.6 \pm 5.6 \mu A/cm^2$ in RL of RYGB $P < 0.05$). The *Glut1* glucose transporter gene, normally
187 barely expressed in mature intestine, was overexpressed in the hyperplastic RL (Figure 3A),
188 but not in the BPL (Figure S4A). GLUT1 immunostaining on mucosa sections from the RL
189 revealed strong basolateral GLUT1 expression both in rats and RYGB-patients (Figure 3C
190 and 3D), showing a similar adaptive response to surgery in human. Interestingly, 40 days
191 after surgery, *Glut1* mRNA levels remained high, but expression of genes encoding SGLT1,
192 GLUT2 and GLUT5 had also increased in the RL (Figure 3B), but not in the BPL (Figure
193 S5B). On the contrary, *Glut3* mRNA remained at a basal level (Figure 3A, 3B, S5A and S5B)
194 and *Glut4* mRNA was never detected in the intestine (not shown). The appearance of GLUT1
195 incited us to measure the expression levels of the hypoxia-inducible genes. *Hif1 α* mRNA
196 increased in the RL and decreased in the BPL 14 days post-surgery in rats (Figure 3A and
197 S5A) whereas the vascular endothelial growth factor *Vegf* mRNA, specifically increased in
198 the RL 40 days after surgery (Figure 3B and S5B).

199

200 **Increase sequestration of glucose in the alimentary Roux limb**

201 We next questioned the functional impact of the modified expression of sugar transporters in
202 the alimentary RL on intestinal glucose handling. We thus performed *ex vivo* transport
203 studies on RL segments of rats subjected to RYGB and jejunal segments of sham-operated

204 rats, with radiolabeled [¹⁴C]-glucose (Figure 4). The time-dependent transport of glucose from
205 the mucosal side to the serosal side (mimicking alimentary glucose absorption) was identical
206 in RYGB and sham groups, and sensitive to phloretin (Figure 4A). However, greater amounts
207 of [¹⁴C]-glucose were found within the RL mucosa after 60min (2,5 fold, $P<0.001$ vs. sham;
208 Figure 4B). The transport of glucose from the serosal side to the mucosal side (mimicking
209 blood glucose transport) was not affected by RYGB surgery (Figure 4C), but again greater
210 amounts of [¹⁴C]-glucose were measured after 60min within the RL mucosa at levels five
211 times higher than that within the sham-operated jejunal segments ($P<0.001$ vs. Sham; Figure
212 4D). *In vivo*, the glycaemic response observed after an oral load of glucose in RYGB-rats
213 was improved as soon as 14 days after RYGB surgery with a similar kinetic of glucose
214 appearance in blood but an accelerated return to normal glycemia, compared to Sham-
215 operated rats or preoperative animals (Figure 4E).

216 We next questioned the physiological relevance of these findings to humans, by reviewing
217 Positron Emission Tomography-Computed Tomography (PET/CT) scan data for individuals
218 that had undergone RYGB surgery. All analysed RYGB patients exhibited abnormal [¹⁸F]-
219 fluorodeoxyglucose ([¹⁸F]-FDG) uptake by the intestine Roux limb. One exhibited a strong
220 hypermetabolic activity in the RL characterized by an intense [¹⁸F]-FDG uptake on
221 attenuation-corrected PET images (Figure 4F and movie S1). The two other RYGB patients
222 had also abnormal [¹⁸F]-FDG uptake by the intestine Roux limb although more limited than
223 the first patient. In comparison, no abnormal uptake was found in the corresponding jejunum
224 of 4 control patients (matched for the body mass index) (Figure 4F and movie S1).

225

226 ***VSG does not induce intestinal hypertrophy but increases number and density of*** 227 ***GLP1-positive cells***

228 We next studied the jejunal remodeling in rats subjected to VSG (Text S2 and Figure S6).

229 Two weeks after surgery, the jejunum was not hypertrophic and its diameter did not change
230 compared with the jejunum of sham-operated rats (Figure 5A). The villus height but not the

231 crypt depth was slightly increased (Figure 5B). The average mucosal area did not change
232 neither after 14 days (Figure 5B) nor after 40 days (Figure S3B). Accordingly, the number of
233 Ki67-positive cells remained similar to that of sham-operated rats (Figure 5C). However, the
234 number and density of GLP1- but not GIP-secreting cells were increased in the jejunum of
235 VSG-operated rat after 14 days (Figure 5D and 5E). Accordingly, plasma GLP1 levels
236 increased 30min after an oral glucose load in VSG-operated compared to sham-operated
237 rats (Figure S4).

238

239 ***VSG does not induce GLUT1 and reduces intestinal absorption of glucose***

240 Contrary to what we observed for hyperplasic RL after RYGB, no change in the expression
241 level of prevalent jejunal sugar transporter occurred after VSG and induction of GLUT1 was
242 detected neither 14 days nor 40 days after the surgery (Figure 6A). Time-dependent glucose
243 transport from the mucosal side to the serosal side (mimicking alimentary glucose
244 absorption) decreased markedly after VSG (Figure 6B). Moreover, the serosal-to-mucosal
245 transport of [¹⁴C]-glucose (mimicking blood glucose uptake) was slightly enhanced (Figure
246 6D). By contrast to RYGB where higher amounts of [¹⁴C]-glucose were measured within the
247 RL mucosa after 60min, the amounts of [¹⁴C]-glucose was not significantly different in the
248 jejunum mucosa of VSG-operated rats (whatever its alimentary or blood origin) (Figure 6C
249 and 6E). *In vivo*, the glycaemic response observed after an oral load of glucose in VSG-
250 operated rats improved, but with both a delayed appearance of glucose in blood (reduced
251 absorption) and an accelerated return to normal, compared to sham-operated or
252 preoperative animals (Figure 6F).

253

254 **DISCUSSION**

255 In this study, using diet-induced obese rats, we directly compared the impact of two bariatric
256 surgeries on the glucose transport capacity of the intestine. We identified two distinct but
257 rapid adaptations affecting intestinal morphology and glucose handling (Figure 7). In
258 response to VSG, glucose transport capacity is reduced and density of cells secreting GLP1
259 is increased. In response to RYGB, the intestine became hyperplastic increasing *de facto* the
260 number of GLP1-secreting cells but more importantly diverting glucose for its own growing
261 needs. Both mechanisms are concomitant with an ameliorated glucose tolerance after
262 surgery. Finally, the physiological relevance of these data was extended to obese individuals
263 after RYGB.

264 It is usually accepted that enterohormones, in particular GLP1, play a role in glycaemic
265 improvement after bariatric surgery ²⁷. In our rat studies, we confirmed that there were no
266 significant changes in the average density of GLP1-producing enteroendocrine cells after
267 RYGB surgery ²¹. The same observations were made in RL from RYGB humans where no
268 variation was observed in the average density of enteroendocrine cells (*i.e.*, Chromogranin
269 A-positive cells) and GLP1 cells. Those results contrast with recent observations made by
270 two different groups reporting an increased GLP1 and GIP cell density one year after RYGB
271 in human ^{28,29}. However, a direct consequence of RL overgrowth after RYGB was a local
272 increase in the number of GLP1- and GIP-producing cells. Thus, even in the absence of cell
273 density modification, the enhanced intestinal mass directly leads to increase the secretory
274 cell population, which in turn could contribute to enhance incretin secretion in response to
275 stimulus as previously reported ^{18,30,31}. Interestingly, in our model of VSG-operated rat, the
276 number and density of GLP1 cells was increased in the jejunum after 14 days. This
277 observation contrasts with recent data showing that the number of GLP1-secreting cells did
278 not change three months after VSG in rats ²¹. Nevertheless it would be a reasonable
279 explanation to the higher rate of GLP1 secretion that we observed with others ¹². Altogether
280 our results suggest an early contribution of GLP1, in the amelioration of glycaemia following

281 surgery, but how the surgeries act on enteroendocrine cell distribution remains controversial.
282 Kinetic analyses would allow determining whether the reported increase in GLP1 and GIP
283 cell density is a transient phenomenon and could explain the discrepancy between early and
284 later stage observations.

285 The hypertrophy of the RL after RYGB was previously reported in numerous rat models ¹⁶⁻²¹.
286 The similar average mucosal area observed 14 and 40 days after surgery in our RYGB rat
287 model suggests that overgrowth of the RL is a very rapid process achieved within two weeks
288 following surgery. The new morphometric characteristics of the RL are maintained over time,
289 for at least one year after surgery in rodents ^{18,19}. This early RL response was characterised
290 by the overexpression of a single sugar transporter, GLUT1, which is normally poorly
291 expressed in mature jejunum ³². GLUT1 has been shown to increase the supply of glucose to
292 proliferative cancer cells in response to hypoxia ³³. Accordingly, levels of mRNA coding for
293 the hypoxia-inducible factor HIF1 were found to have increased in the RL 14 days post-
294 surgery in rats. This suggests that oxygen supply may be insufficient to support the massive
295 hyperplasia. This hypothesis was strengthened by the additional overexpression of *Vegf*
296 mRNA after 40 days. The HIF1 transcription factor directly regulates GLUT1 ^{34,35}. It could,
297 therefore, initiate the reprogramming of glucose metabolism previously reported ^{19,21},
298 providing the required additional energy. Concomitantly to the basolateral appearance of
299 GLUT1, an enhancement of apical SGLT1 activity was measured in the RL of RYGB rats.
300 Thus, apical SGLT1 may act together with basolateral GLUT1 to increase glucose uptake by
301 the RL epithelium and allow energy requirements to be met. Intestinal transport studies
302 revealed that greater amounts of absorbed glucose remained within the RL mucosa
303 suggesting that the alimentary RL increases glucose uptake from the lumen during digestion,
304 and consumes it to satisfy its own energy requirements. The increase in alimentary and
305 circulating glucose uptake and consumption by RL epithelial cells may enhance glucose
306 disposal during and between meals, thereby improving glycaemic control. A previous study,
307 analysing [¹⁸F]-FDG biodistribution in rats ¹⁹, ranked the remodelled intestine as the second

308 highest glucose consumer, after the brain. We next extend those results to humans. Gut
309 hyperplasia following RYGB surgery, with appearance of glucose transporter GLUT1 at the
310 basolateral membrane, leads to an increase in glucose consumption by the RL. The
311 consequent glucose disposal, may contribute to the better glucose tolerance observed in rats
312 and to the resolution of diabetes reported in humans ¹. One limitation of the present study is
313 the small number of patients which renders delicate to draw strong conclusions about human
314 intestinal adaptation. However, GLUT1 overexpression and hypermetabolic activity of the
315 Roux limb observed in RYGB patients at different post-surgical stage provided evidence for
316 the potential physiological relevance of these findings in humans.

317 Whereas the early induction of GLUT1 may be crucial to sustain the energy-consuming
318 overgrowth of the intestine after RYGB, the subsequent overexpression of the other intestinal
319 transporters, SGLT1, GLUT2 and GLUT5, could allow the increase in sugar absorption to
320 counterbalance the malabsorption generated by the intestinal shortening. These two steps of
321 intestinal adaptation processes may make different contributions to the early and long-term
322 effects of RYGB surgery. They could reconcile previous controversial observations about
323 expression patterns of sugar transporters after surgery ^{17,19,22,24}.

324 Compared to RYGB, VSG is a less intrusive intervention involving surgical resection of a
325 large part of the stomach, but results in a similar improvement in fasting glucose
326 concentrations independently of weight loss ^{31,4}. Thanks to low complication rates and short
327 hospital stays, VSG surgery is becoming the most popular bariatric surgery in developed
328 countries. Nevertheless, little is known about its mechanisms of action and, to date, no study
329 investigates the consequences of this surgery on intestinal glucose handling except one
330 recent publication reporting no increase in hexokinase II protein expression after VSG versus
331 RYGB ²¹. Using our rat models, we directly compared and contrasted gut adaptation in
332 response to VSG *versus* RYGB surgery. No hypertrophy of the jejunum mucosa, no
333 induction of GLUT1 and no change in the expression level of prevalent jejunal sugar
334 transporter occurred 14 days or 40 days after VSG. This absence of intestinal hypertrophy,

335 confirmed after three months in a recent study ²¹, shows that an increase in glucose disposal
336 by the hypertrophic intestine is not likely to account neither for short-term nor for long-term
337 improvements in glycaemia triggered by VSG. Consistently, no increase in the sequestration
338 of glucose, whatever its origin (alimentary or blood), occurred in the jejunum of VSG-
339 operated rats. However, the transport of alimentary glucose markedly decreased after VSG,
340 suggesting that VSG jejunum had a lower absorption capacity of alimentary glucose. A slight
341 but significant increase in transepithelial glucose transport from blood to the lumen was also
342 detected. The origin of this regulation is unknown, but VSG may improve glucose tolerance
343 by delaying the entry of alimentary glucose, and possibly by releasing some blood glucose
344 into the lumen. These results were in agreement with the delayed glycaemic response
345 observed after an oral load of glucose in our rats and reported in humans ³⁶. Intestinal
346 remodelling could thus play a major role in the initial improvement of glucose homeostasis
347 following both surgeries not only through better incretin secretion, but also through modified
348 intestinal glucose handling. Another consequence of gastro-intestinal remodelling by bariatric
349 surgery that we did not address in this study is accelerated gastric emptying, although it may
350 be important for incretin secretion and blood glucose delivery ¹¹⁻¹³. More interventional
351 studies in rat models will be required to evaluate the relative contributions of each of these
352 parameters to the regulation of glycemia.

353 **Conclusion**

354 In this study, we report that bariatric surgeries induce profound changes in glucose handling
355 by the intestine although underlying mechanisms differ considerably between VSG and
356 RYGB (Figure 7). In RYGB, alimentary glucose and blood glucose are sequestered by
357 epithelial cells for their own use, whereas, in VSG, the uptake of alimentary glucose by the
358 intestine is reduced. Further studies with more patients are needed to understand whether
359 these adaptive mechanisms are key determinants for diabetes resolution in humans. Our
360 results, nevertheless, unveil the reconfigured intestine as a putative contributor of glycemic

361 improvement and thwart the intuitive idea that RYGB and VSG must share a common
362 mechanism of action for a similar efficiency.

363

364 REFERENCES

- 365 1. Rubino F, Schauer PR, Kaplan LM, et al. Metabolic Surgery to Treat Type 2 Diabetes: Clinical
366 Outcomes and Mechanisms of Action. *Annu. Rev. Med.* 2010;61:393–411.
- 367 2. Pournaras DJ, Osborne A, Hawkins SC, et al. Remission of type 2 diabetes after gastric bypass
368 and banding: mechanisms and 2 year outcomes. *Ann. Surg.* 2010;252:966–971.
- 369 3. Chambers AP, Jessen L, Ryan KK, et al. Weight-Independent Changes in Blood Glucose
370 Homeostasis after Gastric Bypass or Vertical Sleeve Gastrectomy in Rats. *Gastroenterology*
371 2011;141:950–958.
- 372 4. Schauer PR, Bhatt DL, Kirwan JP, et al. Bariatric Surgery versus Intensive Medical Therapy for
373 Diabetes — 3-Year Outcomes. *N. Engl. J. Med.* 2014;370:2002–2013.
- 374 5. Ardestani A, Rhoads D, Tavakkoli A. Insulin Cessation and Diabetes Remission After Bariatric
375 Surgery in Adults With Insulin-Treated Type 2 Diabetes. *Diabetes Care* 2015;38:659–664.
- 376 6. **Isbell JM, Tamboli RA**, Hansen EN, et al. The Importance of Caloric Restriction in the Early
377 Improvements in Insulin Sensitivity After Roux-en-Y Gastric Bypass Surgery. *Diabetes Care*
378 2010;33:1438–1442.
- 379 7. Lingvay I, Guth E, Islam A, et al. Rapid Improvement in Diabetes After Gastric Bypass Surgery.
380 *Diabetes Care* 2013;36:2741–2747.
- 381 8. Lips MA, Groot GH de, Klinken JB van, et al. Calorie Restriction is a Major Determinant of the
382 Short-Term Metabolic Effects of Gastric Bypass Surgery in Obese Type 2 Diabetic Patients.
383 *Clin. Endocrinol. (Oxf.)* 2014;80:834–842.
- 384 9. Sweeney TE, Morton JM. Metabolic surgery: Action via hormonal milieu changes, changes in
385 bile acids or gut microbiota? A summary of the literature. *Best Pract. Res. Clin. Gastroenterol.*
386 2014;28:727–740.
- 387 10. Holst JJ. Enteroendocrine secretion of gut hormones in diabetes, obesity and after bariatric
388 surgery. *Curr. Opin. Pharmacol.* 2013;13:983–988.
- 389 11. Marathe CS, Rayner CK, Jones KL, et al. Relationships Between Gastric Emptying, Postprandial
390 Glycemia, and Incretin Hormones. *Diabetes Care* 2013;36:1396–1405.
- 391 12. Chambers AP, Smith EP, Begg DP, et al. Regulation of gastric emptying rate and its role in
392 nutrient-induced GLP-1 secretion in rats after vertical sleeve gastrectomy. *Am. J. Physiol. -*
393 *Endocrinol. Metab.* 2014;306:E424–E432.
- 394 13. Seeley RJ, Chambers AP, Sandoval DA. The Role of Gut Adaptation in the Potent Effects of
395 Multiple Bariatric Surgeries on Obesity and Diabetes. *Cell Metab.* 2015;21:369–378.
- 396 14. Campbell JE, Drucker DJ. Pharmacology, physiology, and mechanisms of incretin hormone
397 action. *Cell Metab.* 2013;17:819–837.

- 398 15. Mingrone G, Castagneto-Gissey L. Mechanisms of early improvement/resolution of type 2
399 diabetes after bariatric surgery. *Diabetes Metab.* 2009;35:518–523.
- 400 16. Bueter M, Löwenstein C, Olbers T, et al. Gastric Bypass Increases Energy Expenditure in Rats.
401 *Gastroenterology* 2010;138:1845–1853.e1.
- 402 17. Taqi E, Wallace LE, Heuvel E de, et al. The influence of nutrients, biliary-pancreatic secretions,
403 and systemic trophic hormones on intestinal adaptation in a Roux-en-Y bypass model. *J. Pediatr.*
404 *Surg.* 2010;45:987–995.
- 405 18. Mumphrey MB, Patterson LM, Zheng H, et al. Roux-en-Y gastric bypass surgery increases
406 number but not density of CCK-, GLP-1-, 5-HT-, and neurotensin-expressing enteroendocrine
407 cells in rats. *Neurogastroenterol. Motil.* 2013;25:e70–79.
- 408 19. **Saeidi N, Meoli L, Nestoridi E**, et al. Reprogramming of intestinal glucose metabolism and
409 glycemic control in rats after gastric bypass. *Science* 2013;341:406–410.
- 410 20. Hansen CF, Bueter M, Theis N, et al. Hypertrophy Dependent Doubling of L-Cells in Roux-en-
411 Y Gastric Bypass Operated Rats. *PLoS ONE* 2013;8:e65696.
- 412 21. Mumphrey MB, Hao Z, Townsend RL, et al. Sleeve Gastrectomy Does Not Cause Hypertrophy
413 and Reprogramming of Intestinal Glucose Metabolism in Rats. *Obes. Surg.* 2015:1–6.
- 414 22. Stearns AT, Balakrishnan A, Tavakkolizadeh A. Impact of Roux-en-Y gastric bypass surgery on
415 rat intestinal glucose transport. *Am. J. Physiol. - Gastrointest. Liver Physiol.* 2009;297:G950–
416 G957.
- 417 23. Bhutta HY, Deelman TE, Roux CW le, et al. Intestinal sweet-sensing pathways and metabolic
418 changes after Roux-en-Y gastric bypass surgery. *Am. J. Physiol. - Gastrointest. Liver Physiol.*
419 2014;307:G588–G593.
- 420 24. Nguyen NQ, Debreceni TL, Bambrick JE, et al. Upregulation of intestinal glucose transporters
421 after Roux-en-Y gastric bypass to prevent carbohydrate malabsorption. *Obesity* 2014;22:2164–
422 2171.
- 423 25. Fernández-López JA, Casado J, Argilés JM, et al. Intestinal handling of a glucose gavage by the
424 rat. *Mol. Cell. Biochem.* 1992;113:43–53.
- 425 26. **Arapis K, Cavin JB**, Gillard L, et al. Remodeling of the Residual Gastric Mucosa after Roux-
426 En-Y Gastric Bypass or Vertical Sleeve Gastrectomy in Diet-Induced Obese Rats. *PLoS ONE*
427 2015;10:e0121414.
- 428 27. Salehi M, D’Alessio DA. Effects of glucagon like peptide-1 to mediate glycemic effects of
429 weight loss surgery. *Rev. Endocr. Metab. Disord.* 2014;15:171–179.
- 430 28. Rhee NA, Wahlgren CD, Pedersen J, et al. Effect of Roux-en-Y gastric bypass on the
431 distribution and hormone expression of small-intestinal enteroendocrine cells in obese patients
432 with type 2 diabetes. *Diabetologia* 2015:1–5.
- 433 29. **Nergård BJ, Lindqvist A**, Gislason HG, et al. Mucosal glucagon-like peptide-1 and glucose-
434 dependent insulinotropic polypeptide cell numbers in the super-obese human foregut after gastric
435 bypass. *Surg. Obes. Relat. Dis. Off. J. Am. Soc. Bariatric Surg.* 2015.

- 436 30. Papamargaritis D, Miras AD, Roux CW le. Influence of diabetes surgery on gut hormones and
437 incretins. *Nutr. Hosp.* 2013;28 Suppl 2:95–103.
- 438 31. Chambers AP, Jessen L, Ryan KK, et al. Weight-Independent Changes in Blood Glucose
439 Homeostasis after Gastric Bypass or Vertical Sleeve Gastrectomy in Rats. *Gastroenterology*
440 2011;141:950–958.
- 441 32. Thorens B. Glucose transporters in the regulation of intestinal, renal, and liver glucose fluxes.
442 *Am. J. Physiol. - Gastrointest. Liver Physiol.* 1996;270:G541–G553.
- 443 33. Szablewski L. Expression of glucose transporters in cancers. *Biochim. Biophys. Acta BBA -*
444 *Rev. Cancer* 2013;1835:164–169.
- 445 34. Ebert BL, Firth JD, Ratcliffe PJ. Hypoxia and Mitochondrial Inhibitors Regulate Expression of
446 Glucose Transporter-1 via Distinct Cis-acting Sequences. *J. Biol. Chem.* 1995;270:29083–
447 29089.
- 448 35. **Chen C, Pore N**, Behrooz A, et al. Regulation of glut1 mRNA by Hypoxia-inducible Factor-1
449 interaction between H-ras and hypoxia. *J. Biol. Chem.* 2001;276:9519–9525.
- 450 36. Jiménez A, Ceriello A, Casamitjana R, et al. Remission of type 2 diabetes after Roux-en-Y
451 gastric bypass or sleeve gastrectomy is associated with a distinct glycemic profile. *Ann. Surg.*
452 2015;261:316–322.

453

454 **Author names in bold designate shared co-first author.**

455

456 **FIGURE LEGENDS**

457

458 **Figure 1. Hypertrophy and highly proliferative crypt cells in the Roux limb after RYGB**
459 **surgery.**

460 (A and C) Representative images of hematoxylin-phloxine-saffron (HPS)-stained section (A)
461 or Ki67-immunostained section (C) of the alimentary Roux limb (RL) and biliopancreatic limb
462 (BPL) of RYGB-rats and corresponding jejunal segment (Jej) from sham-operated rats 14
463 days post-surgery. Scale bar, 1 mm (A) and 100 μ m (C).

464 (B and D) Morphometric analyses showing the mucosal area, villus height and crypt depth
465 (B) and number of Ki67-immunoreactive cells per crypt (D) in the RL and BPL of RYGB-rats
466 ($n = 4$), and jejunum from sham-operated rats (Jej) ($n = 5$) 14 days post-surgery. Data are
467 means \pm SEM. * $P < 0.05$, ** $P < 0.01$ versus sham, based on ANOVA with Bonferroni
468 correction for multiple comparisons.

469 (E and F) Representative images of HPS-stained (E) and Ki67-immunostained jejunum
470 mucosa section (F) of RL mucosa from a patient who underwent RYGB (right), one year
471 post-surgery, compared to a perioperative jejunum section from an obese individual (left).
472 Scale bar, 500 μ m.

473

474 **Figure 2. Increased number of enteroendocrine cells after RYGB surgery.**

475 (A) Representative images of GLP1 immunostaining in RL and BPL sections from RYGB-rats
476 and jejunum from sham-operated rats 14 days post-surgery. Scale bar, 100 μ m.

477 (B-C) Number of GLP1 (B) and GIP (C) immunoreactive cells per section and per mm² in the
478 RL and BPL of rats after RYGB surgery ($n = 4$) or in the jejunum of sham-operated rats ($n =$
479 5), 14 days post-surgery. Data are means \pm SEM. *** $P < 0.001$ versus sham, in ANOVA with
480 Bonferroni correction for multiple comparisons.

481 (D-E) Representative images of Chromogranin A (D) and GLP1 (E) immunostaining in Roux
482 limb sections from a patient who underwent RYGB (right), one year post-surgery and in the
483 corresponding jejunum sections from an obese subject (left). Scale bar, 200 μm .

484

485 **Figure 3. Early induction of the glucose transporter GLUT1 in the Roux limb after**
486 **RYGB surgery.**

487 (A and B) Relative mRNA levels for sugar transporters and hypoxia-inducible genes in the
488 Roux limb mucosa at (A) 14 days ($n = 4$) or (B) 40 days ($n = 5$) after RYGB. The dotted lines
489 indicate the mean mRNA levels of the corresponding genes in jejunal mucosa from sham-
490 operated rats ($n = 5$). Data are means \pm SEM. * $P < 0.05$, ** $P < 0.01$ versus sham-operated
491 rats, in Mann-Whitney test.

492 (C) Representative images of GLUT1 immunostaining in Roux limb mucosa sections from
493 RYGB-rats and corresponding jejunal sections from sham-operated rats 14 days post-
494 surgery. Scale bar, 50 μm .

495 (D) Representative images of GLUT1 immunostaining in Roux limb sections from a patient
496 who underwent RYGB, one year post-surgery and in the corresponding jejunum mucosa
497 sections from an obese subject. Scale bar, 100 μm (upper panels). High magnification: lower
498 panels. Scale bar 20 μm .

499

500 **Figure 4. Increase in glucose consumption by the alimentary Roux limb after RYGB is**
501 **associated with better oral glucose tolerance.**

502 (A) Time course for the mucosal to serosal transport of [^{14}C]-glucose across the RL of RYGB-
503 rats ($n = 4$) and the corresponding jejunum segment from sham-operated rats with ($n = 3$)
504 and without ($n = 8$) phloretin, 14 days post-surgery.

505 (B) Mucosal [^{14}C]-glucose content of intestine segments at 60 minutes, showing greater
506 sequestration of alimentary glucose within the RL from RYGB-rats ($n = 4$) than within the

507 equivalent jejunal segment from sham-operated rats ($n = 8$). Data are means \pm SEM. *** $P <$
508 0.001, *versus* sham-operated rats, in Mann-Whitney tests.

509 (C) Time course for the serosal to mucosal transport of [^{14}C]-glucose across the RL of
510 RYGB-rats ($n = 4$) and the corresponding jejunum segment from sham-operated rats with (n
511 = 3) and without ($n = 8$) phloretin, 14 days post-surgery.

512 (D) Serosal [^{14}C]-glucose content of intestine segments at 60 minutes, showing greater
513 sequestration of peripheral glucose within the RL from RYGB-rats ($n = 4$) than within the
514 equivalent jejunal segment from sham-operated rats ($n = 8$). Data are means \pm SEM. *** $P <$
515 0.001, *versus* sham-operated rats, in Mann-Whitney tests.

516 (E) Blood glucose levels after an oral load of glucose (1 g/kg) and the corresponding
517 calculated area under the curve (AUC, inset) in obese rats before (preoperative, $n = 12$) and
518 12 days after RYGB ($n = 4$) or sham surgery ($n = 5$). Data are means \pm SEM. * $P < 0.05$, ** P
519 < 0.01 , *versus* the preoperative value, in two-way ANOVA followed by Bonferroni correction
520 for multiple comparisons.

521 (F) Representative images from whole-body [^{18}F]-FDG PET/CT scan of a control individual
522 and a RYGB patient. The blue arrowhead shows a strong [^{18}F]-FDG uptake by the Roux limb
523 in patient who underwent RYGB (yellow-white signal) compared to the undetectable signal in
524 the jejunum of BMI-matched control patient illustrating the hypermetabolic activity of the
525 Roux limb in RYGB patient.

526

527 **Figure 5. VSG does not induce intestinal hypertrophy but increases density and**
528 **number of GLP1-positive cells.** (A) Representative cross-sections of the jejunum of a VSG-
529 rat and a sham-operated rat, 14 days post-surgery. Scale bar, 1 mm.

530 (B) Morphometric analyses of the jejunum showing the mucosal area of sections, villus
531 height and crypt depth from VSG-rats ($n = 5$), compared with sham-operated rats ($n = 5$) 14
532 days post-surgery. Data are means \pm SEM. * $P < 0.05$, NS (not significant), *versus* sham-
533 operated rats, in Mann-Whitney test.

534 (C) Representative images of Ki67-immunostained sections and quantification of Ki67-
535 positive proliferating cells in the crypts of jejunum from rats subjected to VSG or sham
536 surgery, 14 days post-surgery. Scale bar, 100 μm . NS not significant, *versus* sham-operated
537 rats, in Mann-Whitney test.

538 (D-E) Quantification of (D) GLP1 and (E) GIP-immunoreactive cells per section and per mm^2
539 of jejunum sections from VSG-rats ($n = 4$) and sham-operated rats ($n = 5$). Scale bar, 100
540 μm . Data are means \pm SEM. $*P < 0.05$, NS not significant, *versus* sham-operated rats, in
541 Mann-Whitney test.

542

543 **Figure 6. VSG decreases intestinal glucose absorption.** (A) Relative mRNA levels of
544 sugar transporters in the jejunal mucosa from rats subjected to VSG 14 days ($n = 4$) or 40
545 days ($n = 5$) post-surgery. The dotted line indicates the mean mRNA levels in sham-operated
546 rats ($n = 5$). Data are means \pm SEM.

547 (B-D) Time course of mucosal-to-serosal (B) and serosal-to-mucosal (D) [^{14}C]-glucose
548 transport across the jejunum of rats subjected to VSG ($n = 6$) and sham surgery, with ($n = 3$)
549 or without ($n = 8$) phloretin, 14 days post-surgery. Data are means \pm SEM. $*P < 0.05$, $**P <$
550 0.01 , $***P < 0.001$, *versus* sham-operated rats, in two-way ANOVA with Bonferroni correction
551 for multiple comparisons.

552 (C-E) [^{14}C]-glucose content of intestine segments at 60 minutes. No significant difference in
553 the sequestration of alimentary (C) or peripheral (E) glucose within the jejunal segments was
554 observed between VSG and sham-operated rats. Data are means \pm SEM. NS, not
555 significant, in Mann-Whitney test.

556 (F) Blood glucose levels after administration of an oral load of glucose (1 g/kg) and the
557 corresponding calculated area under the curve (AUC, insert) in obese rats before
558 (preoperative, $n = 16$) and 12 days after VSG ($n = 5$) or sham surgery ($n = 9$). Data are
559 means \pm SEM. $^{\#}P < 0.05$ (sham vs. preoperative), $**P < 0.01$, $***P < 0.001$ (VSG vs.
560 preoperative), in two-way ANOVA with Bonferroni correction for multiple comparisons.

561

562 **Figure 7. Schematic view of the differential intestinal adaptations after RYGB and VSG**
563 **leading to improvement of glucose tolerance**

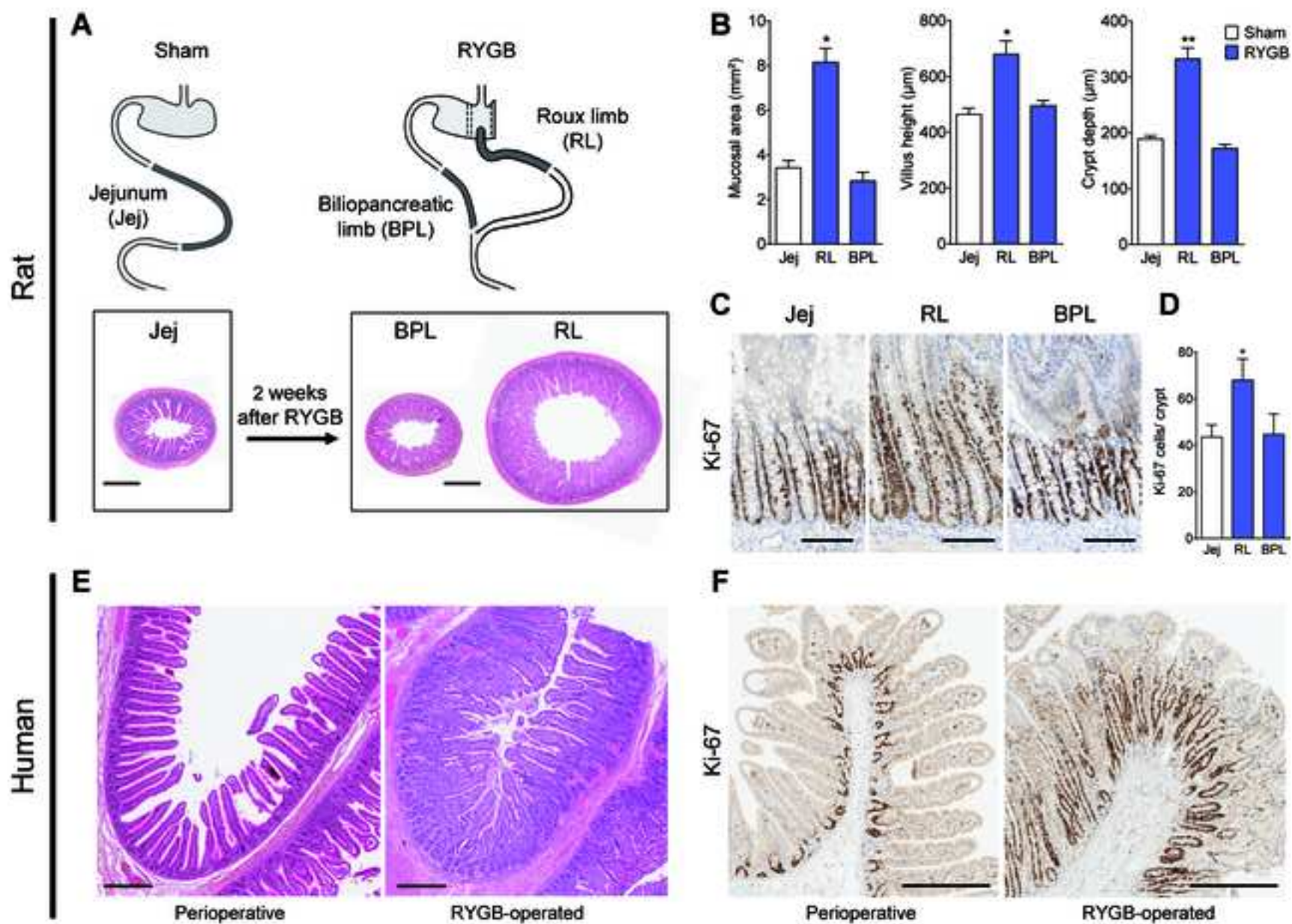
564 In response to RYGB, the intestine became hyperplasic, alimentary glucose transport and
565 blood glucose uptake increased but glucose was sequestered by epithelial cells for their own
566 use. In response to VSG, alimentary glucose transport capacity was reduced and a slight
567 increase in transepithelial glucose transport from blood to the lumen was detected. Both
568 intestinal adaptations contribute to ameliorate sugar tolerance after surgery.

569

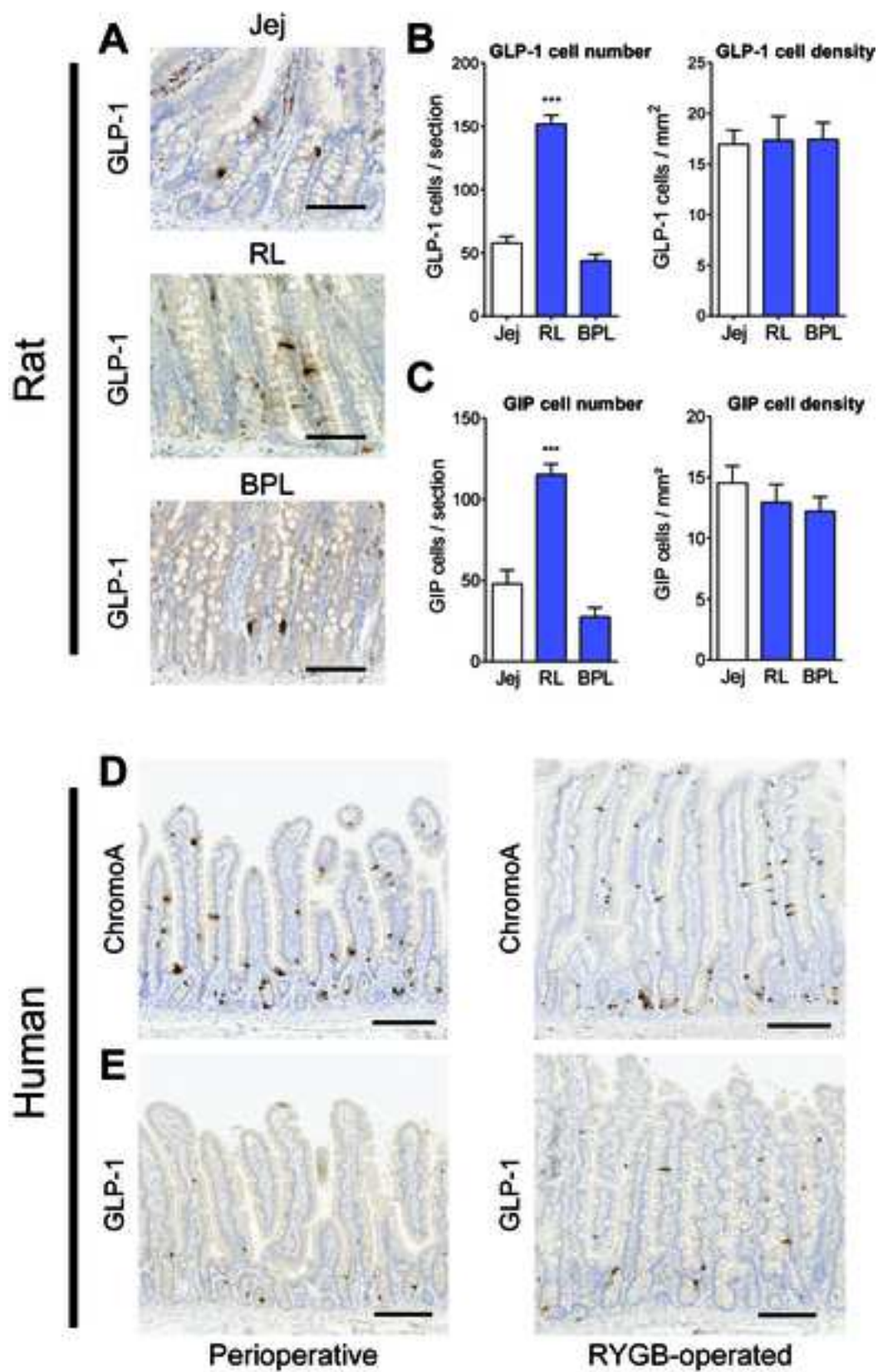
570 **ACKNOWLEDGMENT**

571 We would like to thank the team of N.K. at Department of Functional coprology, APHP for
572 stool analyses; Pr D. Le Guludec responsible of FRIM imaging platform and Chief of the
573 Nuclear Physic Department; O. Thibaudeau and S. Ameur for help in histologic experiments;
574 V. Descatoire for help in histologic analyses; L. Aline for technical help; J. Le Beyec, H.
575 Duboc and S. Ledoux for comments. M.L.G. thanks L. Arnaud for constant support.

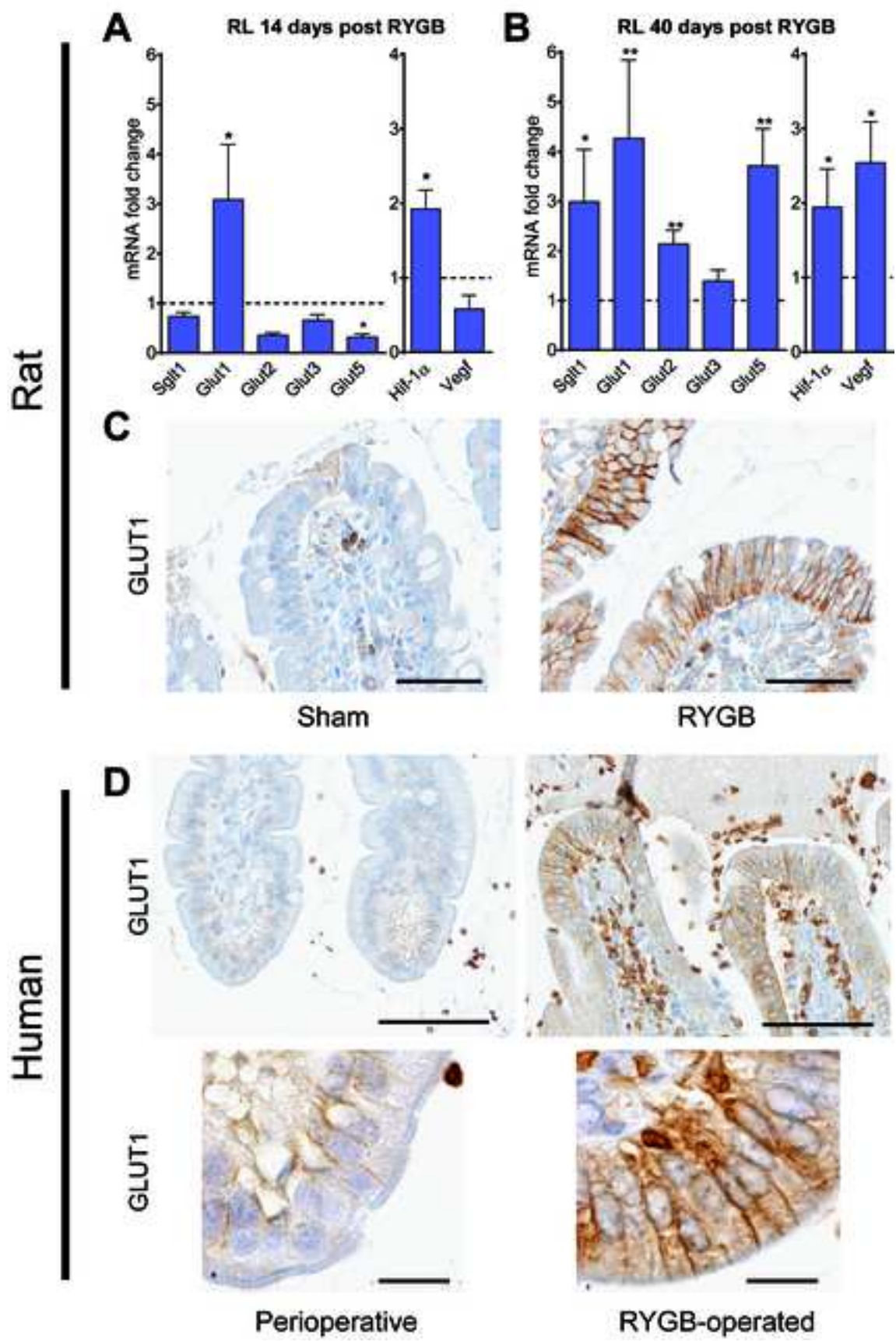
Cavin et al, Figure 1



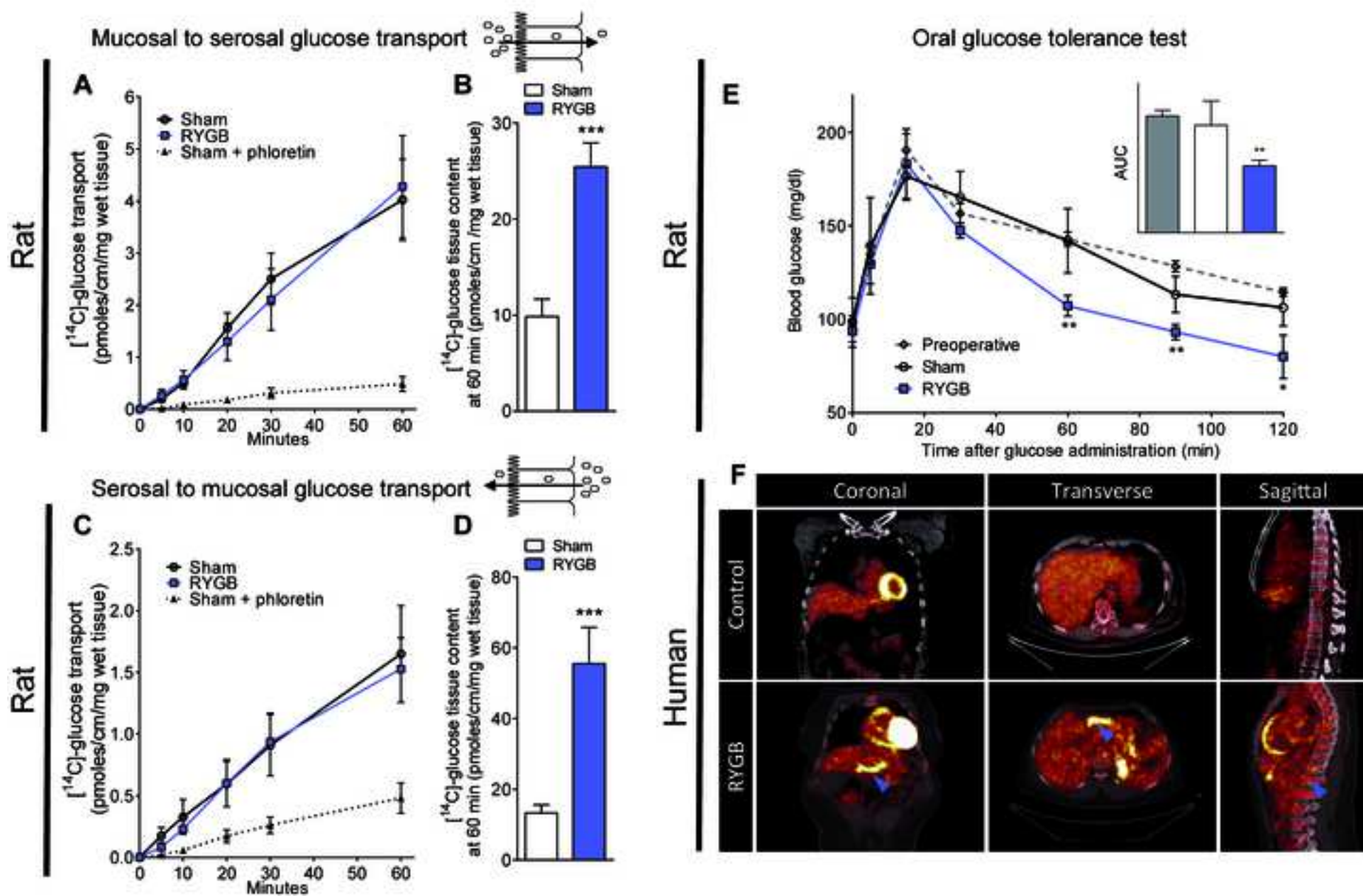
Cavin et al, Figure 2



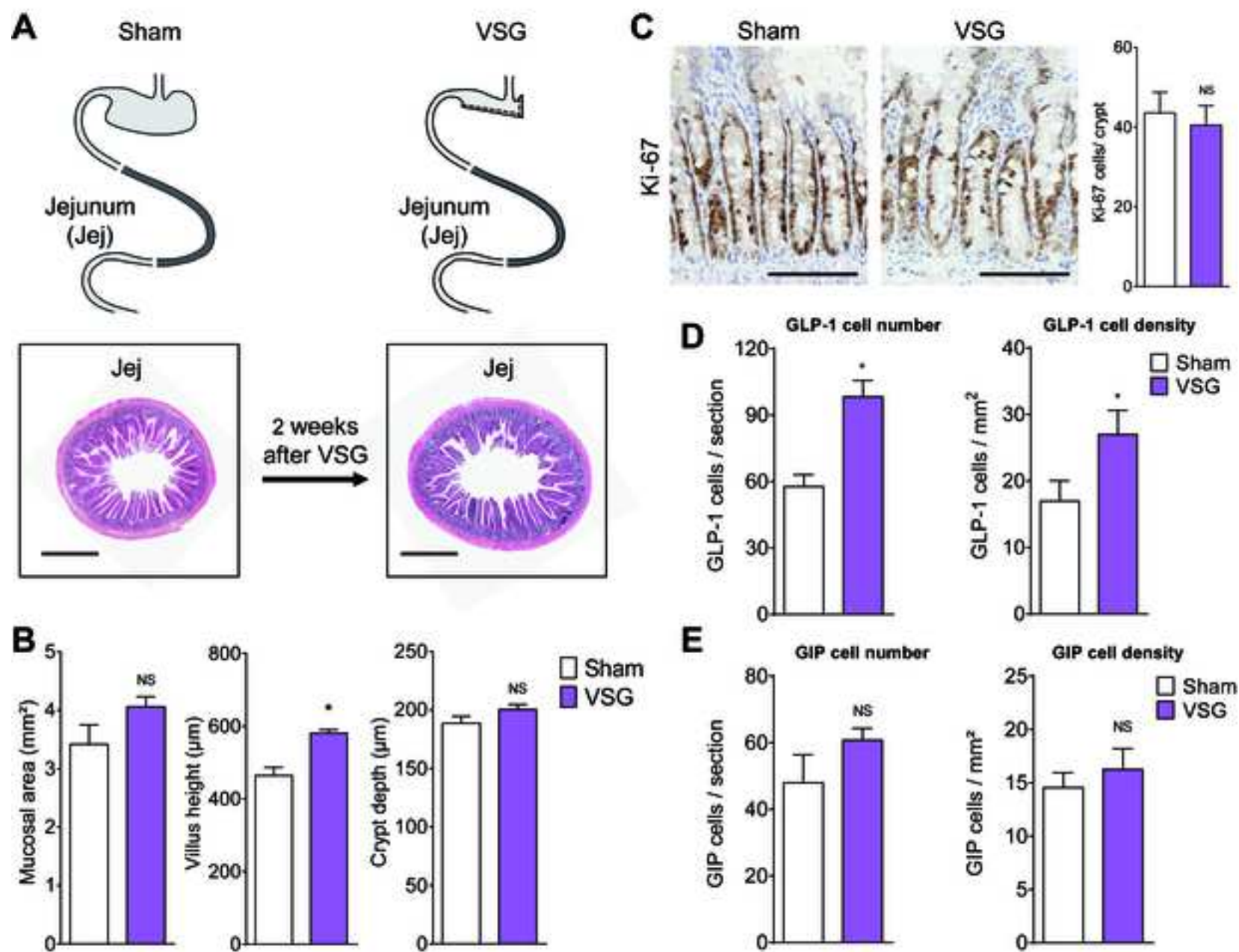
Cavin et al, Figure 3



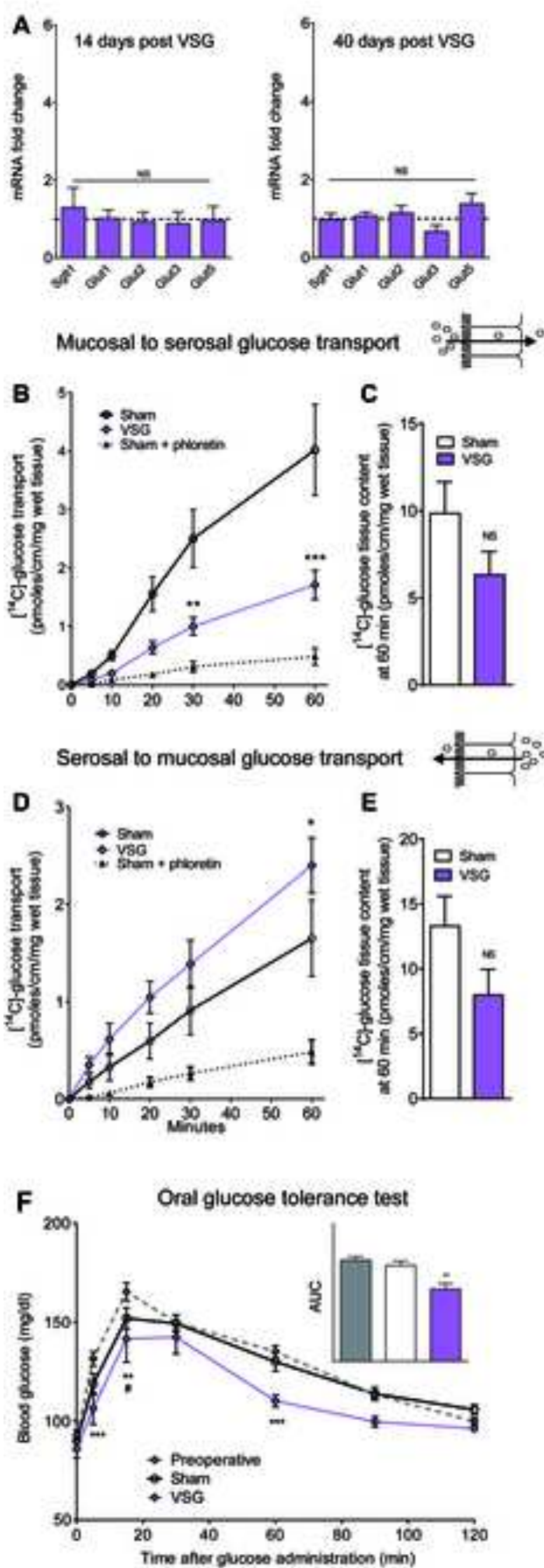
Cavin et al, Figure 4



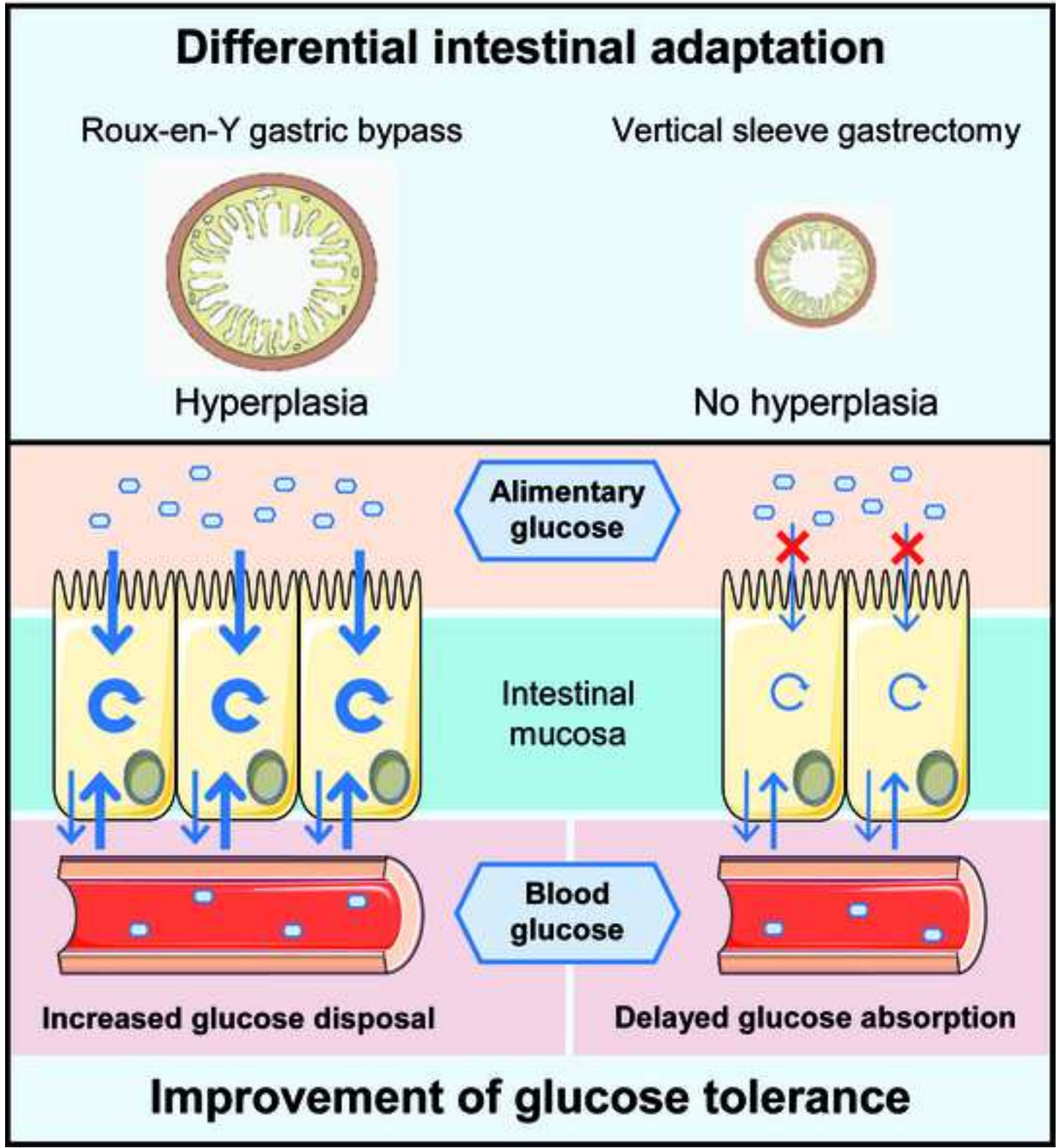
Cavin et al, Figure 5



Cavin et al, Figure 6



Cavin et al, Figure 7



SUPPORTING DOCUMENTS

Supplemental Experimental Procedures

Animal surgeries and post-surgery procedures

Male Wistar rats weighing 220–240 g were fed with high-fat diet (HFD, Altromin C45) for 16 weeks. Diet-induced obese rats weighing 675 ± 50 g were divided into Roux-en-Y gastric bypass (RYGB), sleeve gastrectomy (VSG) and sham-operated (sham) group. They were fasted overnight before operation. Anesthesia was induced by intraperitoneal injection of pentobarbital (Ceva, Libourne, France). Standard aseptic procedures were used throughout. After laparotomy, the stomach was isolated outside the abdominal cavity. Loose gastric connections to the spleen and liver were released along the greater curvature, and the suspensory ligament supporting the upper fundus was severed.

RYGB: The forestomach was resected using an Echelon 45-mm staple gun with blue cartridge (Ethicon, Issy les Moulineaux, France). Then, the gastric pouch was created with a TA-DST 30-mm-3.5-mm stapler (Covidien, Courbevoie, France) preserving the arterial and venous supply. The jejunum was transected 15 cm distally from the pylorus. The Roux limb was anastomosed to the gastric pouch and the biliopancreatic limb was anastomosed 20 cm distally to gastro-jejunal anastomosis with 6-0 Polydioxanone (PDS) running sutures.

VSG: After resection of the forestomach as above, 80% of the stomach was resected with an application of Echelon 45-mm staple gun, leaving a thin gastric tube in continuity with the esophagus and keeping the antrum in place.

Sham: To mimic surgery, stomach was tweaked with an unarmed staple gun for RYGB sham and VSG sham and jejunum was transected and repair for RYGB sham.

For all these procedures, the laparotomy was closed with 5.0 Polyglycolide (PGA) suture in two layers.

Post-operative care:

Health and behavior of each animal were evaluated daily.

RYGB-operated rats were kept without food for 48 h after the surgery. They received subcutaneous injections of 12 mL Bionolyte G5 (Baxter, Maurepas, France) twice a day within this period. From days 3 to 5, they had access to liquid diet (Altromin C-0200, Genestil, Royaucourt, France), which correspond to 50 Kcal/day (50% of preoperative intake). A free access to solid Normal Diet (Altromin 1324, Genestil, Royaucourt, France), was allowed from day 6.

VSG-operated rats were kept without food for 24 h after the surgery but they received subcutaneous injections of 12 mL Bionolyte G5 (Baxter, Maurepas, France) twice a day. From days 2 to 3, they had access to liquid diet (Altromin C-0200, Genestil, Royaucourt, France), which correspond to 50 Kcal/day (50% of preoperative intake). A free access to solid Normal Diet (Altromin 1324, Genestil, Royaucourt, France), was allowed from day 4. Sham-operated rats had the same post-operative care than their corresponding surgical group.

Post-operative analyses: Body weight and food intake were measured daily and the average daily calorie intake was calculated. Fourteen or forty days after surgery, rats were euthanized after overnight food deprivation and gut segments were sampled as illustrated (Figure S1).

Stool analyses

10 days after surgery, rats were transferred into metabolism cages. The total amount of consuming food was recorded each day. The stools were collected daily and stored at -20°C. Stools collected for three days were pooled, and analyses were performed on homogenized samples. Total energy content was determined by bomb calorimetry (PARR 1351 Bomb Calorimeter; Parr Instrument Company). Fecal calorie loss represented the proportion of ingested energy recovered in stool output.

Oral glucose tolerance test

Rats were fasted for 16 h before being subjected to an oral glucose tolerance test (OGTT). Blood was sampled from the tail vein before (t=0) and 5, 15, 30, 60, 90 and 120 min after oral load of glucose (1g/kg body weight). Blood glucose levels were measured with the AccuChek System (Roche Diagnostics, Meylan, France) and expressed in mg/dL.

Plasma GLP1 measurement

Rats were fasted for 16 h before being subjected to an oral load of glucose (1g/kg body weight). Blood (200 μ L), sampled from the tail vein before (t=0) and 30 after the gavage, was collected in presence of DPPIV inhibitor (Roche) to limit degradation of active GLP1. Rat plasma concentrations of active GLP1 was quantified on a Luminex MagPix200 analyzer using Milliplex rat gut hormone panel (RMHMAG-84K Merck Millipore).

Histology and Immunohistochemistry

As a routine process, when obese patients undergo RYGB surgery, a sample is taken from the jejunum in close contact to the anastomosis. When patients are operated on for complication after RYGB, the gastro-jejunal anastomosis is resected and a sample of jejunum is taken 5 cm far from the anastomosis for analyses. RYGB patients were undergoing re-operations for persistent ulcers, dumping syndrome or pouch dilations one to five years after the initial RYGB surgery (Please see TableS 1 for detailed description of the patients). In rats, gut segments were sampled as illustrated (Figure S1) fourteen days or forty days after surgery.

Rat and human samples were immediately fixed overnight in formalin. Three μ m blank slides were cut from each block to perform either hematoxylin phloxine saffron (HPS) staining or immunostaining with Ki67, GLP1, Chromogranin A, GIP and GLUT1 antibodies.

Immunohistochemistry was carried out using an automated immunohistochemical stainer according to the manufacturer's guidelines (Bond-Max autostainer, Leica, Wetzlar, Germany), after dewaxing and rehydrating paraffin sections and antigen retrieval by pretreatment with high temperature at pH 9. After antigen retrieval, tissue sections were immunolabelled with primaries antibodies used as follows: Rat Ki67 (Dako M7248): diluted 1:25, pH6; Human Ki67 (Dako M7240): diluted 1:100, pH9; Rat GLUT1 (spring bioscience E2844): diluted 1:200, pH6; Human GLUT1 (AnaSpec 53519): diluted at 1:200, pH6; Human Chromogranin A (DAKO M0869): diluted 1:250, pH6; Rat GIP (Peninsula Laboratories T-4053): diluted 1:3000, pH6; Rat GLP1 (Abcam AB26278): diluted 1:3000, pH9. Substitution of the primary antibody with PBS was used as a negative control. Subsequently, tissues were incubated with secondary antibody polymer for 10 min (Bond Polymer Refine detection; DS9800; Leica Microsystems) and developed with DAB-Chromogen for 10 min. Internal positive controls consisted in red blood cells for GLUT1 and nucleus of crypt cells for Ki67. Immunostainings were evaluated by two pathologists blinded to the clinical data AC and MH from the department of Pathology of Bichat Hospital. Each slide was scanned with an Aperio ScanScope® CS System (Leica Microsystemes SAS, Nanterre France). Morphometric analyses were performed using the Calopix Software (TRIBVN, Chatillon, France) on three to four distant sections per rat sample. The number of Ki67 immunoreactive cells per crypt was evaluated in 3-4 crypts from three to four cross sections from each intestinal limb for each animal. Averages were used for statistical analyses.

Reverse transcription and Quantitative Real-time PCR

Total RNA was extracted from frozen intestinal mucosa scrapings with TRIzol reagent (Invitrogen, Saint Aubin, France). One µg from each sample was converted to cDNA using the Verso cDNA Synthesis Kit (Thermo Scientific, Waltham, MA, USA). Primers were designed using Roche assay design center or were based on previous studies; they were all synthesized by Eurogentec (Angers, France). Real-time PCR was performed using the Light

Cycler 480 system (Roche Diagnostics, Indianapolis, IN, USA) according to the manufacturer's instructions under the following conditions: 15 min denaturation at 95°C, followed by 50 cycles of 10 sec at 95°C, 45 sec at 60°C and 10 sec at 72°C. Melting curves were performed for each reaction, from 55°C to 95°C at 0.11°C/sec. Ct values of the gene of interest were normalized with two different reference genes (L19 and HPRT) which were chosen after multiple comparisons with numerous reference genes. The primers used in this study are presented below.

Gene	NCBI Accession #	Sequence
<i>Glut1</i>	NM_138827	GTGCTCGGATCCCTGCAGTTCG GGGATGGACTCTCCATAGCGGTG
<i>Glut2</i>	NM_012879	AAAGCCCCAGATACCTTTACCT TGCCCCTTAGTCTTTTCAAGC
<i>Glut3</i>	NM_017102	GCGCAGCCCTTCCGTTTTGC CGCTGGAGGATCTCCGTCCG
<i>Glut5</i>	NM_031741	GCCTTCGGAGTGTCTTGG GGCAGGGACTCCAGTCAG
<i>Hif1α</i>	NM_024359	AAGCACTAGACAAAGCTCACCTG TTGACCATATCGCTGTCCAC
<i>Hprt</i>	NM_012583	GACCGTTCTGTCATGTGCG

		ACCTGGTTCATCATCACTAATCAC
<i>L19</i>	NM_031103	TGCCGGAAGAACACCTTG GCAGGATCCTCATCCTTCG
<i>Sglt1</i>	NM_013033	GAAGGGTGCATCGGAGAAG CAATCAGCACGAGGATGAAC
<i>Vegf</i>	NM_031836	GAGTTAAACGAACGTACTIONTGCAGA TCTAGTTCCCGAAACCCTGA

SGLT1 activity measurement

Intestine segments were opened along the mesenteric border and placed between the two halves of an Ussing chamber (Easy Mount P2312; Physiologic Instrument, San Diego, CA, USA) (exposed area: 0.50 cm²). Tissues were bathed with 4 ml of KRB solution with glucose 10 mM in serosal compartment and mannitol 10 mM in mucosal compartment. Solutions were gassed with 95% O₂–5% CO₂ and kept at a constant temperature of 37°C.

Electrogenic ion transport was monitored continuously as the short-circuit current (I_{sc}) by an automated voltage clamp apparatus (DVC 1000; WPI, Aston, England, UK) linked through a Lab-Trax-4 interface to a computer. Tissue ionic conductance was calculated according to Ohm's law. Sodium-dependent glucose transporter SGLT1 was challenged by 10 mM glucose. Results were expressed as the difference (ΔI_{sc}) between the peak I_{sc} (measured within 10 min) and the basal I_{sc} (measured just before the addition of glucose).

Glucose transport and consumption assay

Glucose transport was assayed *ex vivo* using jejunal loop as described previously¹. Briefly, four 3-cm intestinal segments were filled with Krebs Ringer Bicarbonate Buffer solution containing 30 mM D-glucose with 0.1 $\mu\text{Ci/ml}$ [¹⁴C]-glucose (specific activity 49.5 mCi/mmol) and with or without 100 μM phloretin, a glucose transporter inhibitor. Each segment were ligated at both ends and incubated in a 37°C thermostat-controlled bath of Krebs modified buffer at pH 7.4 continuously gassed with 95% O₂-5% CO₂. Mucosal-to-serosal and serosal-to-mucosal transport of glucose, were monitored using everted and non-everted isolated intestinal loops, respectively. Time dependent [¹⁴C]-glucose transport was determined by sampling from the bath at 0, 5, 10, 20, 30 and 60 min. At 60 min, isolated intestinal loops were collected, flushed, weighed, and homogenized with ultraturax for quantification of radioactivity. Radioactivity was measured using a beta counter (Beckman LS 6000 TA liquid scintillation counter). Apparent permeability (P_{app}) was used to assess transport according to the following equation $P_{app} = (dQ/dt) \cdot (V/Q_0 \cdot A)$, where V is the volume of the incubation medium, A is the area of the loop, Q_0 is the total radiolabeled glucose introduced into the loop and dQ/dt is the flux across the intestinal loop.

Positron emission tomography

Seven patients were retrospectively selected from the files of the department of nuclear medicine, Bichat Hospital, France. Three RYGB patients and four control patients (without gastro-intestinal diseases or cancer) had been evaluated with [¹⁸F]-FDG PET/CT for the detection of workup of thoracic tumours, Horton disease or detection of site of infection or inflammation. The patients were imaged on average 4 years after surgery (Please see Table S2 for detailed description of the patients). PET and CT were performed with a PET/CT hybrid system (Discovery 690; GE Healthcare). Imaging started 60 min after ¹⁸F-FDG injection with a non-enhanced, low-dose CT scan (120 kV, 80 mA), which was followed by a whole-body PET acquisition in 3-dimensional mode with an acquisition time of 4 min per bed

position. PET Imaging was performed only if the fasting glucose level was lower than 7.7 mmol/L before [18F]-FDG injection. Mean glycaemia was 4.9 ± 0.4 mmol/L in the RYGB group and 5.9 ± 1.1 mmol/L in the control group. [18F]-FDG was injected intravenously at a dose of 4 MBq/kg; mean dose was 295 ± 66 MBq in the RYGB group and 361 ± 110 MBq in the control group. [18F]-FDG PET acquisitions were interpreted using the Advantage Workstation of the PET/CT system (GE Healthcare) by two experienced nuclear medicine physicians, who were blinded to the subject's group status. Both physicians worked separately; then, in case of discrepancies, they reviewed the images together in order to reach a consensus. Image analysis was based on visual interpretation and semi-quantitative measurement of [18F]-FDG uptake. On visual analysis, abnormal hypermetabolic activity in the abdominal areas was classified as positive or negative and increased [18F]-FDG uptake in this area was confirmed on non-attenuation-corrected PET images.

Statistical analyses

Statistical analyses were performed with GraphPad Prism version 6.0 (GraphPad Software, SanDiego, CA, USA). Areas under the curves (AUC) were calculated using the trapezoid rule.

Table S1. Patients included for histologic analyses

		Sexe	Age	BMI	Indication for reoperation	Time after RYGB surgery (month)
RYGB operated group*	Patient 1	F	30	37	Persistent ulcer	12
	Patient 2	M	32	36	Dumping syndrome	29
	Patient 3	F	46	38,8	Weight regain and pouch dilation	36
	Patient 4	F	50	39,9	Persistent ulcer	53
	Patient 5	F	56	27,8	Persistent ulcer	60
Obese control group	Patient 1	F	65	54,2	NA	NA
	Patient 2	M	38	49,8	NA	NA
	Patient 3	M	58	61	NA	NA

*None of those patients have experienced intestinal obstruction or any other known issues which could have directly impacted the histologic characteristics of the samples.

Table S2. Patients included for [18F]-FDG PET/CT scan analyses

		Sexe	Age	BMI	Time after RYGB surgery (month)
RYGB operated group	Patient 1	F	54	27,7	48
	Patient 2	F	49	27,8	38
	Patient 3	F	64	33,3	50
Control group	Patient 1	M	73	28,8	NA
	Patient 2	F	80	29,1	NA
	Patient 3	F	56	36,7	NA
	Patient 4	M	49	27,7	NA

Text S1.

To evaluate the histologic and functional adaptation of the alimentary Roux limb after surgery, we performed RYGB in diet-induced obese rats (Figure S2A and S2B). Male Wistar rats fed a high-fat diet for 4 months, were operated and subjected to post-operative care for 6 days before having access ad libitum to solid normal diet. The combination of surgical procedure and postoperative care with liquid diet (caloric restriction) led to a substantial weight loss which was higher in RYGB compared to sham-operated rats (Figure S2C). Weight loss was primarily due to a decrease in food intake (Figure S2D) rather than malabsorption, since fecal calorie loss did not change significantly after surgery (Figure S2E). The incidental role played by malabsorption, compared to decrease in food intake, on weight loss has already been described in few studies^{2,3}. RYGB-operated rats displayed an improved oral glucose tolerance compared to preoperative state at 12 days post-surgery (Figure 4). Caloric restriction during intensive post-operative care period, weight loss and diet switch were not sufficient to trigger improvement of glucose tolerance in sham-operated rats compared to preoperative state (Figure 4). This data highlights the crucial role of surgery on initial post-operative glycemic improvement.

Text S2.

To directly compare the histologic and functional adaptation of the jejunum after VSG and RYGB, we performed VSG in diet-induced obese rats (Figure S6). Operated VSG and Sham rats were subjected to post-operative care for 3 days before having access ad libitum to solid normal diet. The combination of surgical procedure and postoperative care with liquid diet (caloric restriction) led to a substantial weight loss which was higher in VSG compared to sham-operated rats (Figure S6A). Weight loss was primarily due to a decrease in food intake (Figure S6B). Caloric restriction during intensive post-operative care period, weight loss and diet switch were not sufficient to trigger improvement of glucose tolerance in sham-operated rats at 12 days post-surgery compared to preoperative state (Figure 6F). On the contrary,

VSG-operated rats displayed an improved oral glucose tolerance compared to preoperative state at 12 days post-surgery (Figure 6F). This data highlights the crucial role of surgery on initial post-operative glycemic improvement. Of note, the difference in weight loss and food intake in VSG-Sham and RYGB-Sham rats is due to difference in post-operative care. VSG-Sham rats had access to normal food as soon as 4 days post-surgery and lost less weight than sham RYGB-Sham rats who had access to normal food ad libitum only after 6 days post-surgery (Figure S2C and S6A). However, jejunal adaptation and intestinal glucose handling 2 weeks post-surgery were not different between RYGB-Sham and VSG-Sham confirming that weight loss and caloric restriction *per se* were not responsible for intestinal adaptation and improved glucose tolerance observed after RYGB or VSG.

Figure S1. Sampling of intestinal segments

Figure S2.

(A) Postmortem macroscopic views of rat stomach 14 days after sham (upper panel) or RYGB surgery (lower panel). The RYGB procedure results in ingested food flowing from the esophagus (oe) to the gastric pouch (g.po) and then directly to the jejunum (jej) of the Roux limb, bypassing the distal stomach (d.st), the duodenum (du), and part of the proximal jejunum.

(B) Postmortem view of the gastrointestinal tract of a rat after RYGB surgery, showing the lengths of the Roux limb, biliopancreatic limb (which drains gastric, hepatobiliary and pancreatic secretions), and common limb after RYGB with, in continuity, the cecum and the colon. The red dotted line indicates the new path followed by food.

(C) Loss of body weight after surgery in RYGB- (n = 11) and sham-operated rats (n = 9). The black box corresponds to the period of postoperative care (5 days) before the animals had free access to solid normal diet. The data shown are means \pm SEM.

(D) Changes in daily calorie intake after surgery. The dotted line indicates mean calorie intake before surgery. The data shown are means \pm SEM. **P < 0.01, ***P < 0.001, versus preoperative value, in Mann-Whitney tests.

(E) Loss of fecal calories, determined by bomb calorimetry analyses of stools collected on day 12 after surgery. Results are expressed as a percentage of calorie intake.

Figure S3.

(A) Morphometric analyses showing the mucosal area of RL and BPL sections of rats subjected to RYGB surgery (n = 5), compared with the corresponding jejunum segment from sham-operated rats (Jej) (n = 5) 40 days after surgery. Data are means \pm SEM. **P < 0.01 versus sham-operated rats, based on ANOVA with Bonferroni correction for multiple comparisons.

(B) Morphometric analyses showing the mucosal area of sections from VSG-rats ($n = 5$), compared with the corresponding jejunum segment from sham-operated rats ($n = 5$) 40 days after surgery. Data are means \pm SEM. NS, not significant, in Mann-Whitney tests.

Figure S4.

Plasma active GLP1 levels in fasted rats (A) or 30min after an oral load of glucose (1g/kg) (B) 12 days after RYGB ($n = 5$) VSG ($n = 4$) or sham surgery ($n = 3$). Data are means \pm SEM. $*P < 0.05$ (vs. sham), in two-way ANOVA with Bonferroni correction for multiple comparisons.

Figure S5.

(A and B) Relative mRNA levels of sugar transporters and hypoxia inducible genes in the biliopancreatic limb mucosa (A) 14 days ($n = 4$) and (B) 40 days ($n = 6$) after RYGB. The dotted line indicates the mean mRNA level of the corresponding genes in jejunal mucosa from sham-operated rats ($n = 5$). Data are means \pm SEM. $*P < 0.05$, versus sham-operated rats, in Mann-Whitney tests.

Figure S6.

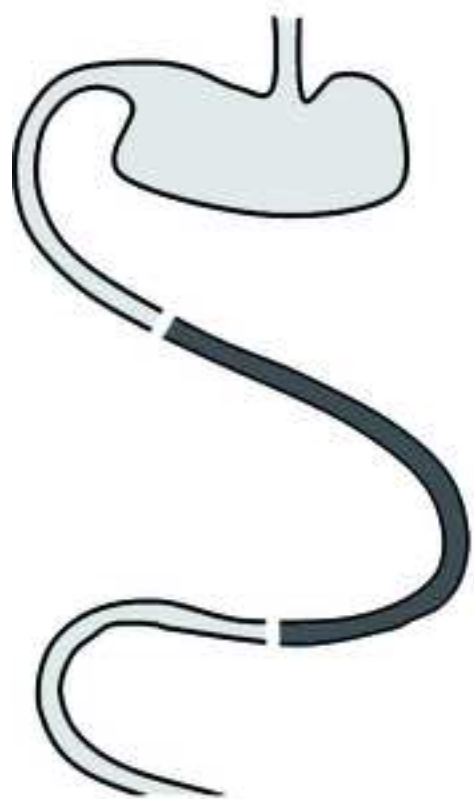
(A) Loss of body weight after surgery in VSG- ($n = 9$) and sham-operated rats ($n = 7$). The black box corresponds to the period of intensive postoperative care (3 days) before the animals had free access to solid normal diet. The data shown are means \pm SEM.

(B) Changes in daily calorie intake after surgery. The dotted line indicates mean calorie intake before surgery. The data shown are means \pm SEM. $***P < 0.001$, versus preoperative value, in Mann-Whitney tests.

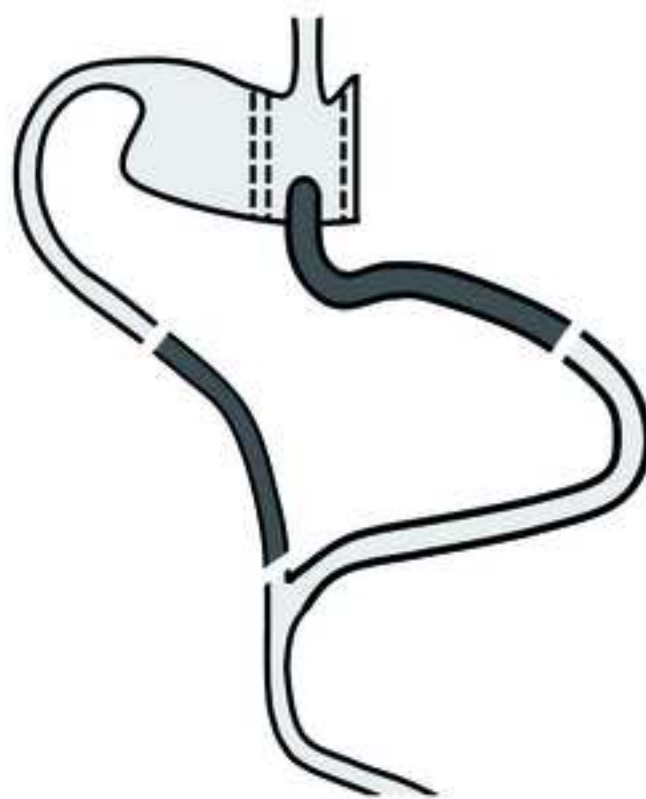
Supplemental References

1. Tavernier A, Cavin J-B, Gall ML, et al. Intestinal deletion of leptin signaling alters activity of nutrient transporters and delayed the onset of obesity in mice. *FASEB J.* 2014;28:4100–4110.
2. Odstrcil EA, Martinez JG, Ana CAS, et al. The contribution of malabsorption to the reduction in net energy absorption after long-limb Roux-en-Y gastric bypass. *Am. J. Clin. Nutr.* 2010;92:704–713.
3. Sandoval D. Bariatric surgeries: beyond restriction and malabsorption. *Int. J. Obes.* 2011;35:S45–S49.

Cavin et al, Figure S1



Sham

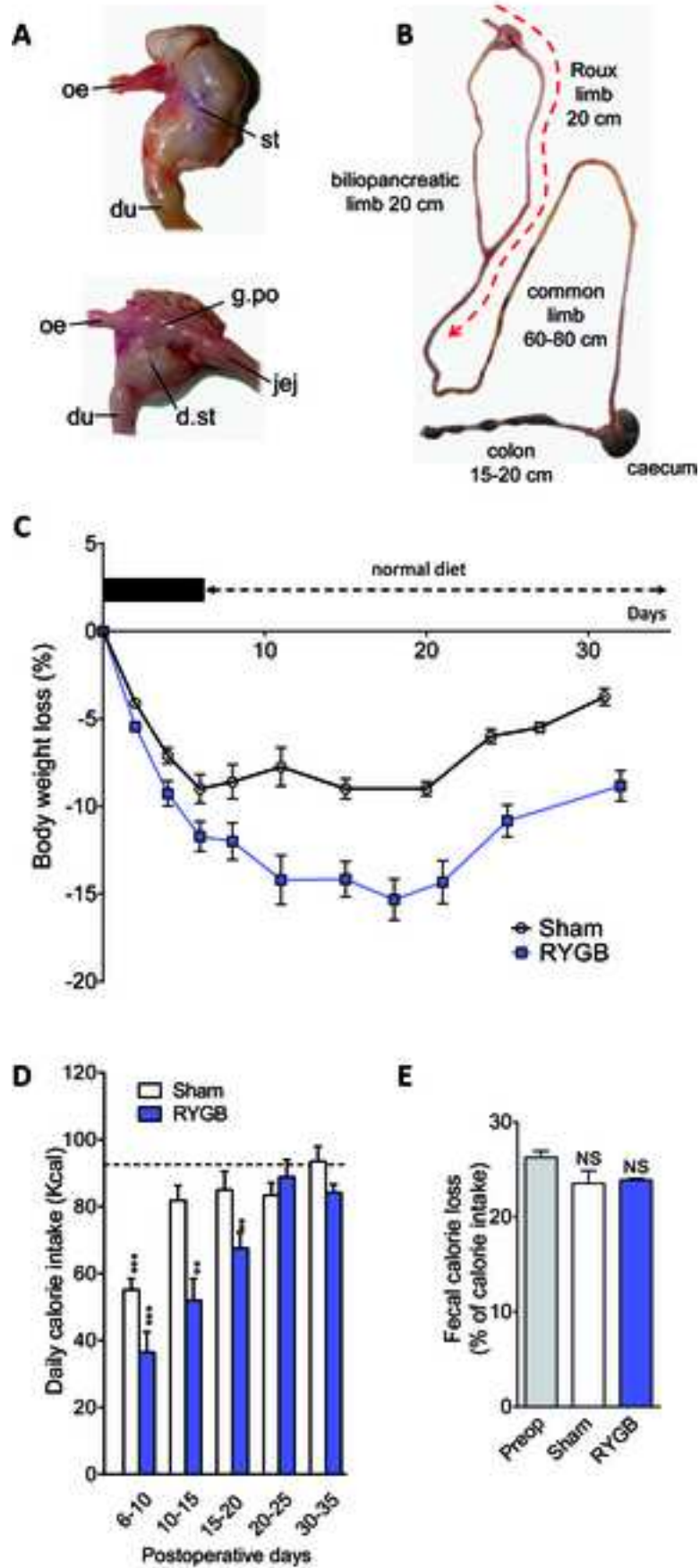


RYGB

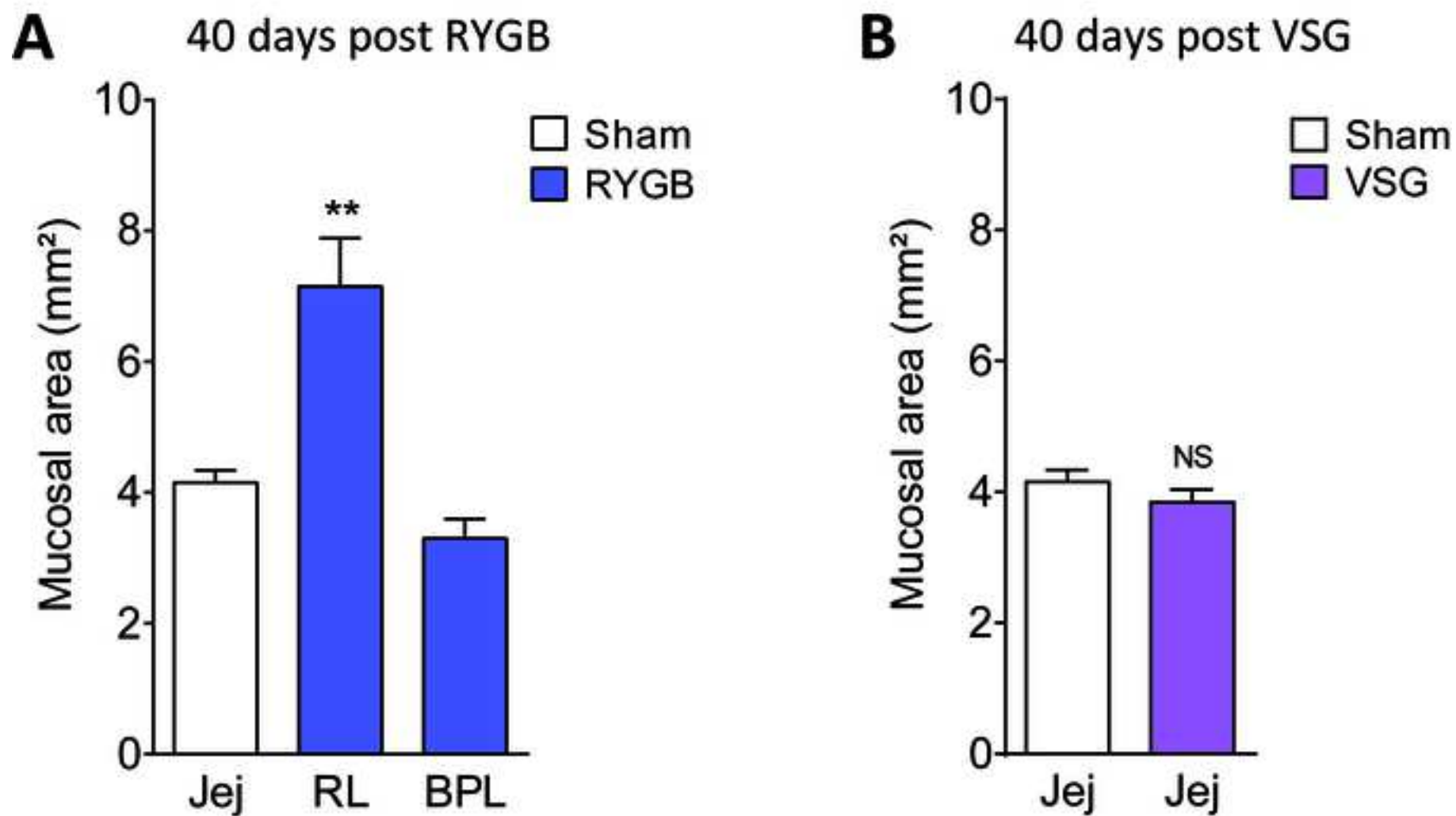


VSG

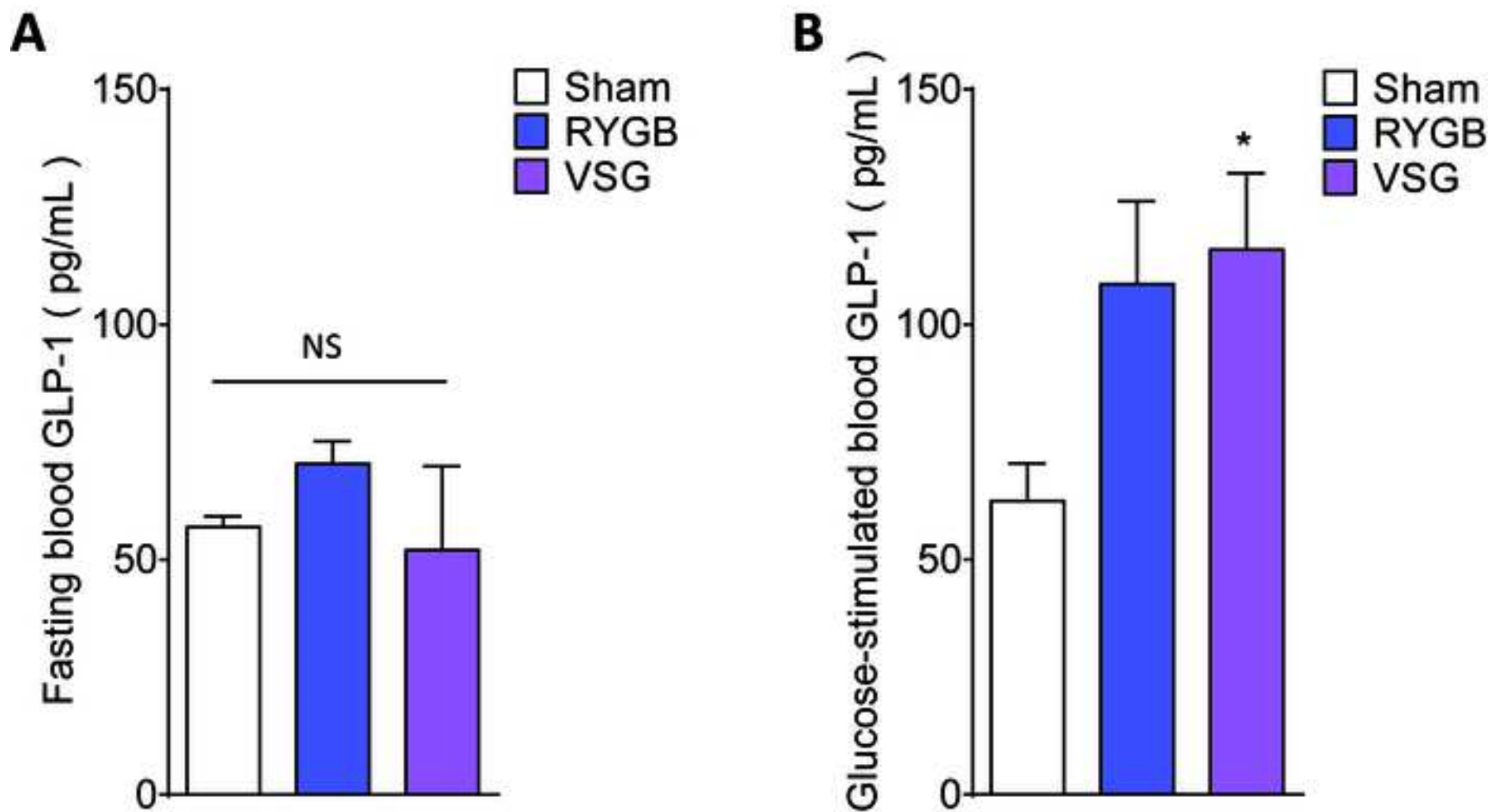
Cavin et al, Figure S2



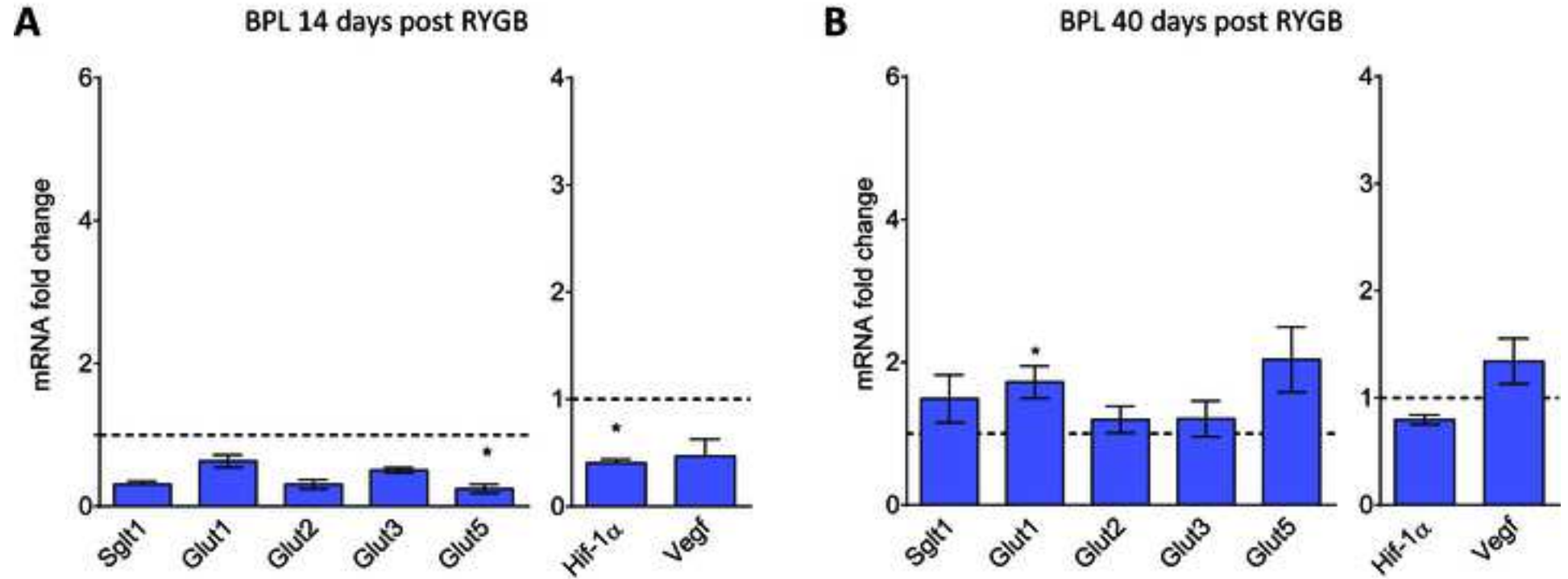
Cavin et al, Figure S3



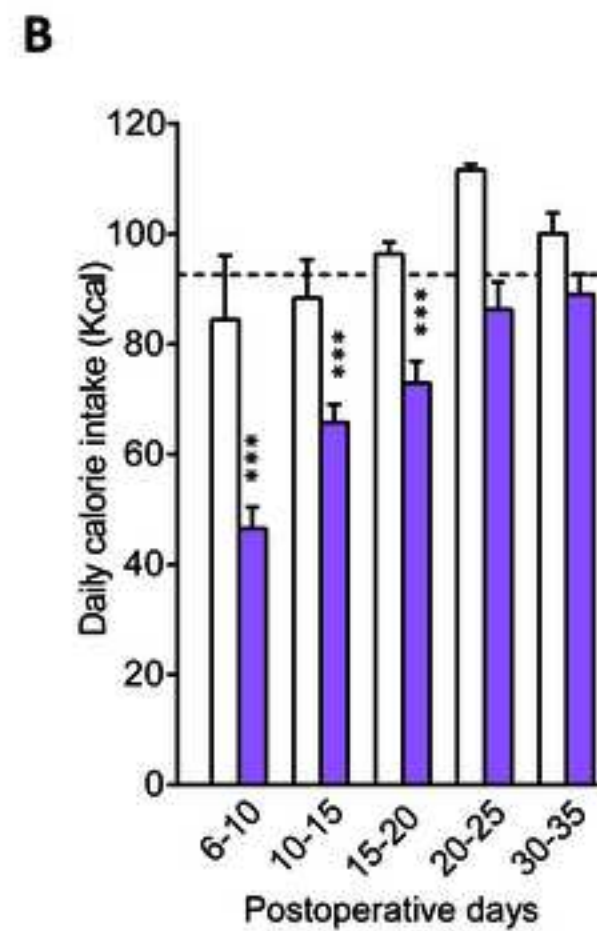
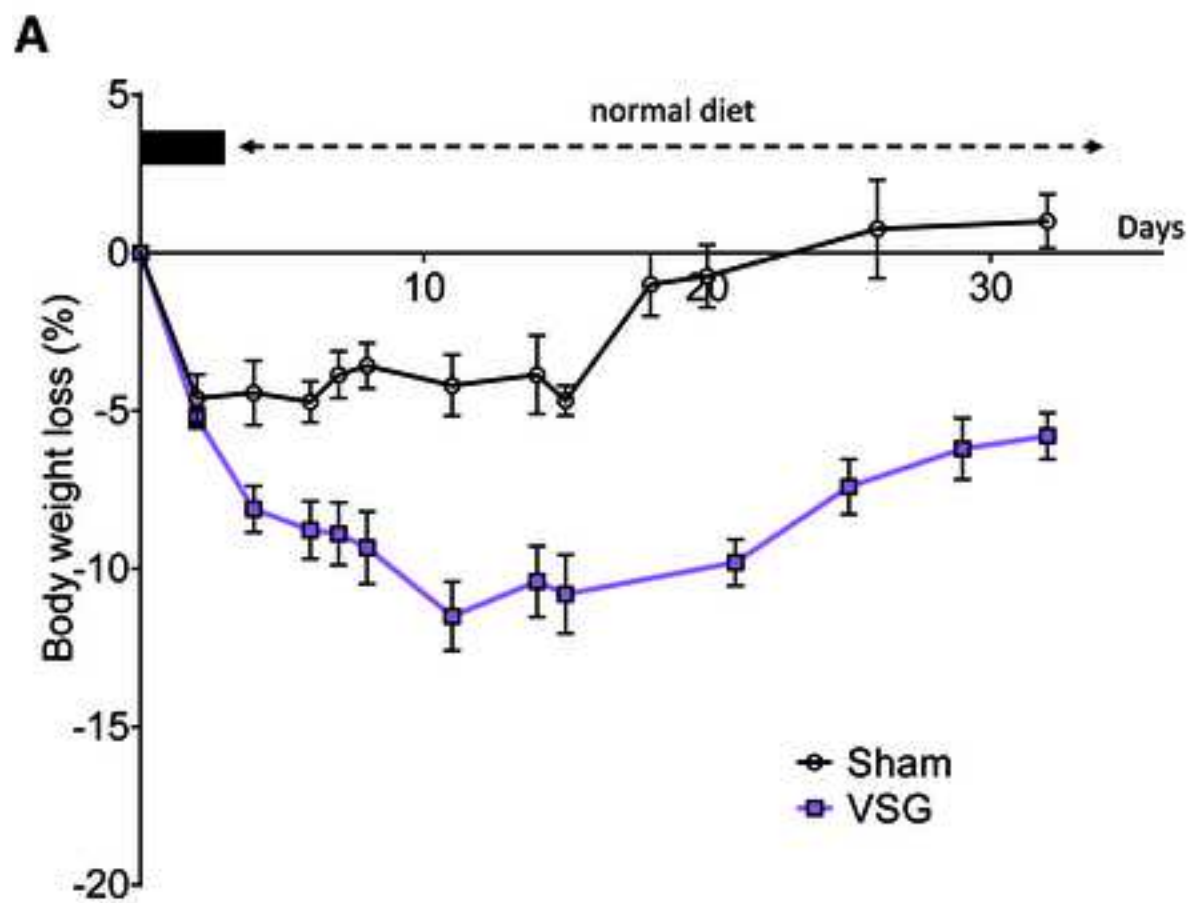
Cavin et al, Figure S4



Cavin et al, Figure S5



Cavin et al, Figure S6



Movie S1

[Click here to download Video \(supplemental\): Movie S1.mp4](#)

Revised Manuscript in Word or RTF (no changes marked)

[Click here to download Revised Manuscript in Word or RTF \(no changes marked\): Revised Manuscript Cavin et al. NO tracked changes.doc](#)